National Library of Canada

Acquisitions and Bibliographic Services Branch

395 Wellington Street
Ottawa, Ontario
K1A 0N4

Bibliothèque nationale du Canada

Direction des acquisitions et des services bibliographiques

395, rue Wellington
Ottawa (Ontario)
K1A 0N4

Your file Votre référence

Our file Notre référence

NOTICE

The quality of this microform is heavily dependent upon the quality of the original thesis submitted for microfilming. Every effort has been made to ensure the highest quality of reproduction possible.

If pages are missing, contact the university which granted the degree.

Some pages may have indistinct print especially if the original pages were typed with a poor typewriter ribbon or if the university sent us an inferior photocopy.

AVIS

La qualité de cette microforme dépend grandement de la qualité de la thèse soumise au microfilmage. Nous avons tout fait pour assurer une qualité supérieure de reproduction.

S'il manque des pages, veuillez communiquer avec l'université qui a conféré le grade.

La qualité d'impression de certaines pages peut laisser à désirer, surtout si les pages originales ont été dactylographiées à l'aide d'un ruban usé ou si l'université nous a fait parvenir une photocopie de qualité inférieure.

Canada

Performance of Organo-clay-PDMS Membranes in Pervaporation Processes

By

Jinhua Bai

A thesis submitted to the School of Graduate Studies

in partial fulfillment of the requirements for

the degree of Master of Science in Chemistry

Department of Chemistry

University of Ottawa

Ottawa, Canada

April, 1995

ISBN 0-612-11538-0

Canada

UNIVERSITÉ D'OTTAWA
UNIVERSITY OF OTTAWA

ACKNOWLEDGMENTS

I would like to thank Professor Christian Detellier, my research supervisor, for his invaluable advice, excellent guidance, much needed support and encouragement throughout my studies.

I wish to express my gratitude to Dr. T. Matsuura for sharing his membrane expertise with me. Thanks is also given to Professor J. Dickson for providing the opportunity of undertaking pervaporation experiments.

I am indebted to my group-mates for the pleasure that they have brought me during my studies and our invaluable discussions.

I would like to thank Ms. C. Bensimon and Dr. J. Blixt for their great help with X-ray diffraction measurements and computer processing, respectively.

Finally, I would like to thank the Institute of Chemical and Scientific Technology for financial support.

Abstract

The objective of this work is to improve the pervaporation separation characteristics of polydimethylsiloxane (PDMS) membranes by imbedding organo-clay particles in the polymer structure.

Montmorillonite is a clay mineral with a 2:1 layered structure. The negative charges on its layers due to the compositional inhomogeneities are counterbalanced with inorganic cations. Organo-montmorillonite is formed when the inorganic cations are exchanged with organic cations. The nature, type and structure of exchangeable cations on montmorillonite strongly influence their sorptive characteristics. Different combinations of these factors will produce very different interlayer environments.

Tetraphenylphosphonium (TPP) and tetraalkylammonium cations (TAAn; where n is the number of carbon of the chain) were intercalated into montmorillonite to form a series of organo-clays (TPP-M; TAAn-M). The organo-clay-PDMS composite membranes (TPP-M-PDMS; TAAn-M-PDMS) were prepared by adding the organo-clays into the PDMS solution. The organo-clays and organo-clay-PDMS composite membranes were characterized by XRD, BET and TGA. The X-ray diffraction results show that the interlayer spacing of the prepared organo-clays ranged from 4 to 9 Å. The microporosity of organo-clay was measured by nitrogen adsorption. The degree of microporosity depends on the nature, size and structure of the cation. The thermal stability of organo-clay-PDMS can reach 400°C.

Pervaporation experiments of dilute 1,2-DCE and benzene solutions were performed

using organo-clay-PDMS composite membranes. The effects of the nature of organo-clays, of the organo-clay content, and of the temperature and downstream pressure as operating variables on the membrane performance were investigated. The results show that the flux and separation factor depend on the nature of the organo-clay, of the organo-clay content and of the organic components in feed solution. It was possible to concentrate benzene three fold in permeate with TPP-M-PDMS membranes due to the high benzene adsorption proportion of TPP-M. This was attributed to the hydrophobic nature of the TPP-M organo-clay. In the case of TAA1-M-PDMS membrane, however, the separation factor decreased and became even lower than the one obtained with organo-clay free PDMS membrane.

The transport mechanism for particle filled PDMS composite membranes was not fully elucidated. A resistance model based on solution-diffusion transport mechanism was used to fit the pervaporation data. The transport phenomena in pervaporation processes with organo-clay-PDMS composite membranes are more complex than in the case of polymer membranes or polymer composite membranes.

TABLE OF CONTENT

LIST OF FIGURES

LIST OF TABLE

SYMBOLS AND ABBREVIATIONS

SWY-1	montmorillonite, from Clay Spur Wyoming USA

Organic cations:

TPP^+	tetraphenylphosphonium, $^+P(Ph)_4$
$TAA1^+$	tetramethylammonium, $^+N(CH_3)_4$
$TAA3^+$	tetrapropylammonium, $^+N(C_3H_7)_4$
$TAA4^+$	tetrabutylammonium, $^+N(C_4H_9)_4$
$TAA5^+$	tetrapentylammonium, $^+N(C_5H_{11})_4$
$TAA6^+$	tetrahexylammonium, $^+N(C_6H_{13})_4$
$TAA7^+$	tetraheptylammonium, $^+N(C_7H_{15})_4$

Organo-clays:

TPP-M	TPP-montmorillonite
TAA1-M	TAA1-montmorillonite
TAA3-M	TAA3-montmorillonite
TAA4-M	TAA4-montmorillonite
TAA5-M	TAA5-montmorillonite

TAA6-M	TAA6-montmorillonite
TAA7-M	TAA7-montmorillonite

Organo-clay and organo-clay polymeric composite membranes:

PDMS	polydimethylsiloxane
Na-M	sodium-montmorillonite
Na-M-PDMS-40	40%(w/w) Na-M in PDMS membrane
TPP-M-PDMS-20	20%(w/w) TPP-M in PDMS membrane
TPP-M-PDMS-30	30%(w/w) TPP-M in PDMS membrane
TPP-M-PDMS-40	40%(w/w) TPP-M in PDMS membrane
TPP-M-PDMS-47	47%(w/w) TPP-M in PDMS membrane
TAA1-M-PDMS-20	20%(w/w) TAA1-M in PDMS membrane
TAA1-M-PDMS-30	30%(w/w) TAA1-M in PDMS membrane
TAA1-M-PDMS-40	40%(w/w) TAA1-M in PDMS membrane
TAA1-M-PDMS-47	47%(w/w) TAA1-M in PDMS membrane
TAA2-M-PDMS-50	50%(w/w) TAA2-M in PDMS membrane
TAA3-M-PDMS-50	50%(w/w) TAA3-M in PDMS membrane
TAA4-M-PDMS-50	50%(w/w) TAA4-M in PDMS membrane
TAA5-M-PDMS-50	50%(w/w) TAA5-M in PDMS membrane
TAA6-M-PDMS-20	20%(w/w) TAA6-M in PDMS membrane
TAA6-M-PDMS-30	30%(w/w) TAA6-M in PDMS membrane

TAA6-M-PDMS-40	40%(w/w) TAA6-M in PDMS membrane
TAA6-M-PDMS-50	50%(w/w) TAA6-M in PDMS membrane
TAA7-M-PDMS-50	50%(w/w) TAA7-M in PDMS membrane
TAA1-M-PDMS-45	45%(w/w) TAA1-M in PDMS membrane
MMDA-M-PDMS-45	45%(w/w) MMDA-M in PDMS membrane

D	diffusion coefficient
α	separation factor
ß	enrichment factor
X_f	mole fraction of organic compound in feed
X_p	mole fraction of organic compound in permeate
P	permeability
J	permeation rate (flux)
A	Cross sectional surface area of the membrane available for permeation
l	Thickness of membrane through which the component permeates
Δp	partial pressure difference
I	current
E	difference in electric potential
R	resistance
n	number of particles
Φ_c	organo-clay content in organo-clay-PDMS composite membrane
Φ_p	PDMS content in organo-clay-PDMS composite membrane

BET	Brunauer-Emmet-Teller
p/p^0	relative pressure of gas
V	volume of N_2 adsorbed
V_m	monolayer capacity
A_m	average area occupied by a molecule of adsorbate in the monolayer
TGA	Thermogravimetric analysis
XRD	X-ray diffraction
d_{001}	basal spacing
d_{av}	average of d value
d_{is}	interlayer spacing
CEC	cation exchange capacity
S_c	unit charge area
S_i	internal surface

Chapter 1

Introduction

1.1 Introduction to clay chemistry

Clays are naturally occurring minerals, composed of aluminate and silicate networks arranged in various ways.[1] Clay minerals may be either non-expandable or expandable. The non-expandable clays can be described as rigid three-dimensional arrangements of the aluminate and silicate groups. The expandable clays have layered structures which can be described by two-dimensional sheets of silicon-oxygen tetrahedra and two dimensional sheets of aluminum oxygen-hydroxyl octahedra.[2] Those sheets allow a solvent such as water to enter between them, thus separating the sheets. In most clay minerals, the tetrahedral and octahedral sheets are superimposed in different fashions to form the clay layers. Each sheet of an expandable clay consists of one or more sheets of tetrahedral silicate ($[SiO_2]^n$, Si atoms occupying the tetrahedral cavities of two sheets of packed O atoms) and one or more sheets of octahedral aluminate ($[Al_XO_Y]_n$, Al atoms occupying some or all of the octahedral cavities between two sheets of packed O atoms). Two common groups are: 1:1 and 2:1 clays. The

1:1 clay minerals consist of repeat layers which are made up of one tetrahedral sheet and one octahedral sheet. The 2:1 clay minerals consist of layers which are made up of one octahedral sheet sandwiched in between two tetrahedral layers. Figure 1.1 shows the molecular structure of a 2:1 clay.

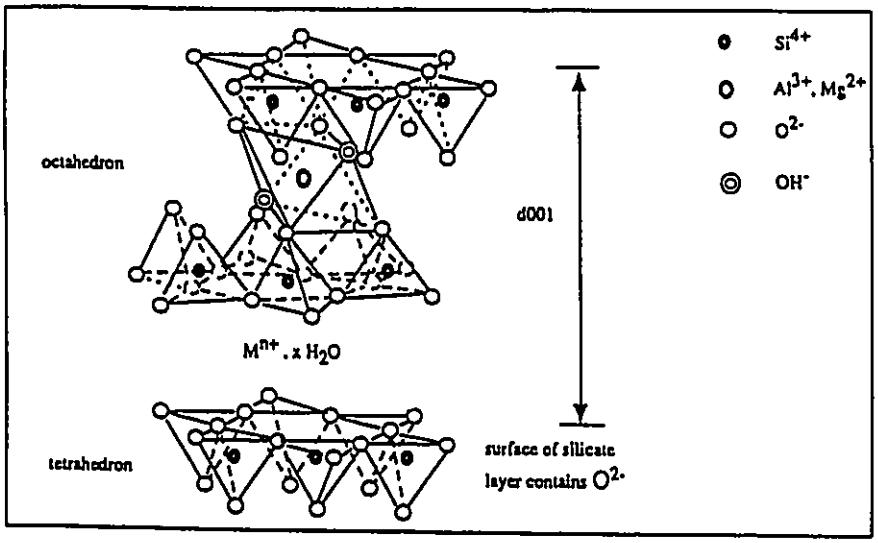

Figure 1.1 Schematic representation of a 2:1 layered clay

What makes clays particularly interesting to chemistry are: (a) the existence of a net negative charge on their layers due to compositional inhomogeneities,[3] (b) the nature of their interlayer spacings which is the distance between two clay layers in a stack.

The negative charge of the clay layer is counterbalanced by adsorbed or intercalated exchangeable cations. In nature, these are usually a mixture of alkali and alkaline earths

metal cations. These are called exchangeable cations because they can be replaced by other cations from a solution. The extent of isomorphous substitution and therefore the magnitude of the layer charge, is determined by the clay cation exchange capacity (CEC), the amount of adsorbed cations needed to neutralize it. The determination of the CEC for an organic clay is essential in order to ascertain the complete exchange of counter-cation with the organic cations. The layer charge in octahedrally charged clays is distributed over all oxygens in the framework.

In the case of an expandable clay, the distance between two clay layers can vary. The insertion of various cations between its layers may force different interlayer spacings. That means that the interlayer spacing is not a fixed value for expandable clays. The increased interlayer spacing can be due to about one layer of hydrocarbon chains between the sheets of the clay mineral. It could also be due to exceptionally large molecules (with long carbon chains) which force a bilayer expanded interlayer spacing. The dependence of interlayer structure on hydrocarbon chain length and clay layer charge density has been discussed by Lagaly.[4] X-ray diffraction is an ideal method by which the interlayer spacing of organo-clay can be determined.

Montmorillonite belongs to the family of smectites, which are expandable clays with 2:1 structure, consisting in a planar three-layer aluminosilicate lattice stacked vertically.[5] Through the isomorphic replacement of aluminum for silicon and magnesium for aluminum there is an excess net negative charge on the lattice, which is satisfied by the presence of inorganic cations (Ca^{2+}, Na^{+}, K^{+}, etc.) situated within the layers, together with water molecules, which form a hydration sphere around the cations.

It should be noticed that montmorillonite may have widely differing cation substitutions, depending on where it was located and under what conditions it was formed.[6] The montmorillonite used in this study is of the SWy-1 variety (a sodium montmorillonite), originating from Clay Spur, Wyoming. It has a high cation-exchange capacity (CEC) and forms a stable thixotropic gel in water.[7] Table 1.1 shows some data for montmorillonite used in this study.[8,13]

Table 1.1 Basic data for SWy-1 montmorillonite

Origin	Clay Spur, Wyoming
Formula	$[Al_{3.22}Fe^{3+}_{0.26}Mg_{0.40}Fe^{2+}_{0.12}](Si_{7.84}Al_{0.16})O_{20}(OH)_4X^{+}_{0.68}$
CEC (meq/100g)	83
Surface area (m^2/g)	740
Density (g/ml)	2.54

1.2 Organo-clays and their application for the removal of organic compounds from water

Organo-clays are formed when the clay counter-balanced cations are exchanged with organic cations. Organo-clays are interesting complements to sorbents such as zeolites because their sorption selectivities can be controlled to a large extent by the choice of layer charge density, structure and the type of exchangeable cations. Different combinations of these factors will produce very different interlayer environments, containing polar mineral surface, hydrophobic organic chains and paraffin-like layers. These materials have been studied as selective sorbents in general,[9-10,14] in gas chromatography,[8] membrane gas

separation[12] and for toxic waste removal.[15-17]

In the past few years, there has been increasing interest in designing recyclable inorganic adsorbents for the efficient removal of organic pollutants from aqueous solutions.[28-29] The hydrophobic character of organo-clay makes them interesting for removal of organic compounds from water. In nature, the net negative charges of clays are usually balanced by inorganic ions, such as Na^+ and Ca^{2+}, which are strongly hydrated in the presence of water. The hydration of these exchangeable metal ions and the presence of Si-O groups in clays gives a hydrophilic nature to the mineral surface. As a result, the adsorption of organic compounds by clays is suppressed in the presence of water because relatively non-polar organic compounds can not effectively compete with highly polar water for adsorption sites on the clay surface. In the absence of water, the clay acts as a conventional solid adsorbents. The high adsorptive capacity for organic compounds is attributed to its large surface area.[18-20]

The intercalation of organic cations into swelling clays has been intensively studied. The inability of clays to remove substantial amounts of organic compounds from aqueous solution can be remedied by replacing natural metal cations with larger organic cations through ion-exchange reactions.[21-23] Earlier studies indicated that exchanging quaternary ammonium cations for metal ions on clays greatly modified the sorptive characteristics of dry clay for organic vapors.[11,24,25] Depending on the size of the organic cations, the exchanged organic ions have been shown to form either a microscopic organic phase, as in hexadecyltrimethylammonium-smectite,[26] or discrete organic-modified surface adsorption sites as in tetramethylammonium-smectite.[10,26] The presence of organic cations in the interlamellar spaces reduces the hydration of the clay and decreases the free aluminosilicate

mineral surface area (i.e.. that surface not covered by the organic ions). As a result, the surface properties of the clay may change considerably from highly hydrophilic, when the clay contains mainly inorganic cations, to increasingly organophilic as the inorganic cations are progressively replaced by organic cations. Therefore, the sorption properties of organic compounds are very favored. Organo-clays can offer preferential sorption of non-polar and flat organic molecules.

Chlorinated hydrocarbons represent one of the most challenging classes of priority pollutants to be removed from waste streams and ground waters.[27,33] The removal of trace levels of pollutants from large volumes of wastewater is a microseparation process requiring cost-effective adsorbents.[16] Modified clay adsorbents have been considered as suitable materials for such applications due to the hydrophobic properties of organo-clays[14,27]. The hydrophobic character as well as the adsorption specificity of those organo-clays allow the potential design of new chromatographic separation and organic pollutant cleanup technologies. It has been found that the uptake of phenol and chlorophenols from water was enhanced by modified clays exchanged with large quaternary alkyl ammonium cations.[31] A study by Lee et al.[14] has shown that montmorillonite exchanged with tetramethylammonium cations was highly effective for the removal of benzene from water. This unique selective property of tetramethylammonium (TAA1)-montmorillonite was attributed to the coordinated water molecules which modifies TAA1-M's sorptive behavior by shrinking the interlamellar cavities, in which adsorption of the aromatic molecules occurred. The study of Yan and Bein et al.[30] demonstrated that a trimethyloctadecylammonium (TrMOA) with trimolecular intercalation shows rapid and substantial uptake of toluene and CH_2Cl_2 from water. It has

been also reported that addition of cetyl pyridinium cations to form a aluminium-pillared montmorillonite resulted in an effective adsorbent for removing pentachlorophenol and benzo(a)pyrene from aqueous solution.[17] Moreover, such aluminium-pillared clays modified by the addition of non-ionic surfactants have been found to exhibit interesting adsorption properties with regard to chlorinated phenols.[31]

1.3 Membrane materials and pervaporation processes

Membrane pervaporation is a rapidly emerging technology for separation of many organic/aqueous systems.[32,33] Pervaporation processes can be grouped into the following general categories:

1. Water removal from organic liquids
2. Removal of organics from water
3. Organic/organic separations
4. Vapor permeation.

Over the past decade membrane pervaporation has gained acceptance by chemical industries as an effective process tool for separation and recovery of liquid mixtures. The number and the variety of industrial pervaporation plants have dramatically increased. However, membrane processes became commercially available only around 1989 for selective permeation of organics from aqueous streams. Because of the associated requirements for good chemical and thermal stability in solvents, most hydrophobic membrane materials, those which are most selective to organics, are not compatible. Currently available composite materials that have been developed for this application are a

compromise, with good chemical properties but limited separation abilities. Although various polymeric materials have been considered, most applied development has focused on the well-known polydimethylsiloxane (PDMS or silicon rubber). In order to improve the separation characteristics of PDMS membrane, various membrane preparation techniques have been applied. PDMS composite membranes, combining a thin and dense PDMS layer with a substrate layer, gives good permeation rates with only a small decrease in selectivity. Recently, the introduction of fillers, such as zeolites with hydrophobic character, into PDMS membranes has been recommended. Several studies with zeolite filled PDMS membranes have shown positive results for removal of organic compounds from aqueous solutions.[34-39]

1.4 The goals of the research

In view of the above mentioned facts, it is possible to introduce organo-clays into PDMS membranes to improve its separation characteristics. The objectives of the present work was to design organo-clay-PDMS composite membranes and to test them for the removal of volatile organic compounds in aqueous solution by pervaporation processes. Organo-clays (TPP-M and TAAn-M) were prepared and characterized by XRD, BET and TGA methods. Organo-clay-PDMS composite membranes were prepared by mixing the organo-clays with polydimethylsiloxane. The efficiency of those composite membranes for pervaporation of 1,2-dichloroethane/water and benzene/water mixtures was determined. Scheme 1.1 gives a very brief overview of the research approach.

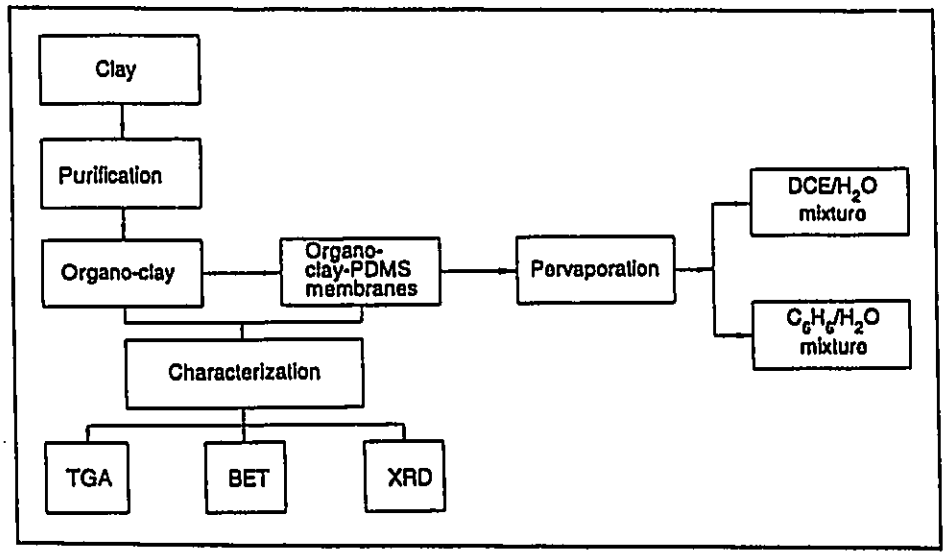

Figure 1.2 A brief overview of research approach

Chapter 2

Pervaporation

2.1 Introduction

Membrane processes have wide industrial applications covering many existing and emerging uses in the chemical, petrochemical, petroleum, environmental, water treatment, pharmaceutical, medical, food, dairy, beverage, paper, textile, and electronic industries. The existing applications include dialysis, electrodialysis, reverse osmosis, ultrafiltration, and microfiltration. Since membrane processes generally have low capital investment, as well as low energy consumption and operating cost, there are a number of emerging applications, which include: gas separation, pervaporation, emulsion liquid membrane, and membrane reactors.[32,33]

Over the past ten years membrane pervaporation has gained acceptance by the chemical industry as an effective process tool for separation and recovery of liquid mixtures. It is currently best identified with dehydration of liquid hydrocarbons to yield high-purity organics. Due to its favourable economics, efficacy, and simplicity, it can be easily integrated into distillation and rectification processes, and even replace them.

2.2 Background

Pervaporation is characterized by the imposition of a barrier (membrane) layer between a liquid and a vapor phase, with mass transfer occurring selectively across the barrier to the vapor side. Because of the unique phenomenon of phase change required for the liquid solutes diffusing across the membrane (permselective "evaporation" of liquid molecules), the process is termed pervaporation.

The early history of development in pervaporation has been sporadic with little continuity. Kober at the New York State Department of Health's research laboratories[40] described an observation that "a liquid in a collodion bag, which was suspended in the air, evaporated, although the bag was tightly closed". Subsequently, Kober coined the term "pervaporation" in 1917. Kober described the experiments for water selective permeation from albumin/toluene solution through collodion bag (cellulose nitrate). Farber at the University of Toronto[41] presented the results of work using pervaporation for concentrating protein solution in 1935. Heissler et al.[42] published their findings on dehydration of aqueous ethanol solutions through regenerated cellulosic membranes in 1956.

The commercial potential of pervaporation for separating azeotropic mixtures and for the separation of organic mixtures was recognized by Binning et al..[43] Pervaporation was proposed as an industrial separation process. For example, dehydration of ethanol by pervaporation has been commonly used in industrial application. Traditional ethanol distillation consists of two parts: (a) normal distillation to 95% ethanol and (b) azeotropic distillation to 99.5% (anhydrous ethanol). This azeotropic distillation is a rather energy consuming process compared to the normal distillation part. Benzene has been used as an

azeotropic dehydrating agent in many plants, but there are concerns existing about its carcinogenicity and toxicity. From those points, pervaporation is considered to be a useful and economical process to produce high purity ethanol.

Many of the further studies were focused on separation of organic mixtures commonly found in petrochemical processing with cellulosic and poly(ethylene) membranes. Despite the intensive investigations by Binning and coworkers, their attempts to introduce pervaporation as an industrial process were not successful. The main reasons for this failure was insufficient permeation rate and/or selectivity for commercial applications.

This situation changed in the sixties when the phase-inversion procedure was developed by Loeb and Sourirajan[44-46] to manufacture high flux, asymmetric, reverse osmosis cellulose acetate membranes. It suddenly became clear that the low permeability of dense polymeric materials was not an insuperable obstacle and that the use of asymmetric or composite barriers could make it possible to exploit the high selectivity of pervaporation transport.

The earliest mention of an operating pilot-plant dates back to 1982.[47,48] This information concerned a small demonstration unit installed in Brazil by the German Company called G.F.T. (Gesellschaft für Trenntechnik, Honburg/Saar, F.R.G.), and which was used to obtain the dehydration of water-ethanol mixtures issued from the predistillation of broths resulting from the fermentation of biomass. The membrane used for this separation was a composite membrane consisting of three layers. An ultrafiltration poly(acrylonitrile) membrane was supported on a non-woven fabric. A very thin layer of crosslinked poly(vinylalcohol) was further coated on the top of the poly(acrylonitrile) membrane.[49] Since

then, a number of composite membranes have been developed by the GFT[50] company, each exhibiting good selectivity (10 to 1000) for a specific separation.

Meanwhile, multiple membrane options were developed, all based on novel proprietary asymmetric composite polymer technologies for producing economical, chemically and thermally stable membranes in a flat plate geometry. Other experiments were made by companies newly introduced in the market of pervaporation, such as Membrane Technology and Research, Inc., (U.S.A.) and KALSEP (U.K.). Their tests focused on the removal of volatile organic solvents contained in waste water[51] with a composite proprietary membrane, consisting of a microporous layer and a thin, dense organophilic coating on the top of the microporous layer.

In recent years, there has been an increase in the use of pervaporation processes for separation of organic components from water.[52] This feature is of great interest in many applications, such as the treatment of organically contaminated waste water,[53] the harvesting of organic substances from fermentation broths,[54] and the recovery of valuable organic components from process side-steams.[55]

Currently pervaporation research and development are taking place on a worldwide basis. The main research is focused on the study of the transport mechanisms through the membrane as well on the selection and the synthesis of new materials for membranes combining high permeability with high selectivity.

2.3 Definitions and fundamentals of the pervaporation

Pervaporation differs from other membrane processes in that the membrane

constitutes a barrier between the feed in the liquid phase and the permeate in the vapor phase. In this technique the feed is circulated in contact with a polymeric membrane and the permeate is evolved, in the vapor state, from the opposite side of the permselective membrane which is kept under vacuum by continuous pumping (vacuum-pervaporation) or swept by a stream of inert gas (sweeping gas pervaporation). The permeate thus obtained is finally collected in the liquid state after condensation on a cooled wall. A schematic diagram of a pervaporation process is shown in Figure 2.1.

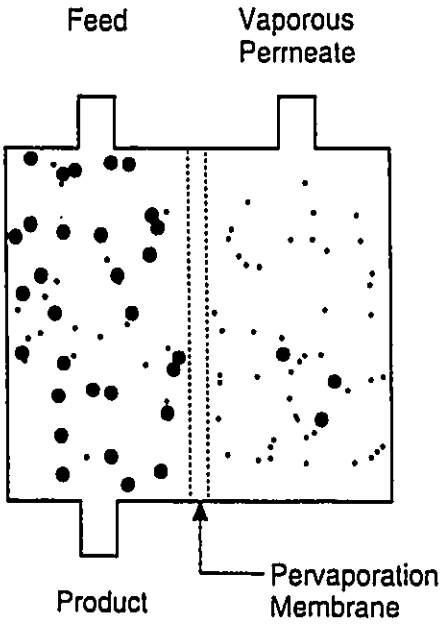

Figure 2.1 Schematic diagram of a pervaporation process

In recent studies on the separation mechanisms of pervaporation, there are different opinions on how selectivity and transport could be explained. A thorough discussion of

transport theory and models for pervaporation is given by Aptel and Neel[56] and others. A summary of the available transport studies is presented in this section.

A majority of transport studies are based on the conventional solution-diffusion model. This model considers the transport process in pervaporation as three successive steps: first, the penetrant molecules are sorbed from the feed liquid phase into the polymeric membrane, then, they diffuse through the membrane, and finally they are desorbed on the downstream side.

The driving force applied across the membrane for this separation creates a chemical potential gradient in the liquid phase, and the selectivity of the membrane is then the determining factor in the relative flow of the different components.[32] According to the solution-diffusion mechanism, the driving force for the transport is generally recognized as gradient in chemical potential between the liquid and the vapor. As each component of the feed dissolves in the membrane, then diffuses across the membrane to the permeate side, the flux of each component is given by

$$J_i = -D_i c_i [d(\mu_i/RT)]/dx \qquad (2\text{-}1)$$

For pervaporation, the activity gradient across the membrane far exceeds the pressure gradient, so that Eq. (2-1) can be rewritten as

$$J_i = -D_i c_i [d(\ln a_i)]/dx \qquad (2\text{-}2)$$

Equation (2-2) demonstrates that the diffusion coefficient, D_i, and activity, a_i (i.e., concentration), are the most important factors in controlling the separation. It must be noticed that different versions of the solution diffusion model exists in the literature. These models differ in their assumptions concerning the transport through the pervaporation.

Beside the solution-diffusion model, other models are also used to describe the transport through the pervaporation. Binning et al.[43] classified pervaporation membranes as non-porous films. They suggested that the selectivity took place in a boundary layer between the liquid zone and the vapor zone in the membrane. The liquid zone of membrane may be visualized as a highly swollen state of polymer in which there is a high concentration of permeating liquid in the polymer structure. The gas zone in which the evaporation of liquid occurs, may be considered as a region in which permeating molecules are much more dispersed and the polymer structure corresponds nearly to the dry polymer film. The existence of two completely different phases within the film seems quite reasonable because the opposite surfaces of the film are subjected to such different conditions. It was proposed that little selectivity occurs at the liquid-membrane interface, but most of the selectivity occurs at the interface between the liquid phase and the vapor phase. The diffusion in the latter zone was believed to be the rate determining step in the process.

Michaels et al.[57] interpreted the selectivity as a result of sieving by the polymer crystals. Schrodt et al.[58] suggested that hydrogen bonding between polymer and solvent components play an important role. Long[59] considered that the diffusion and concentration gradients in the different solvent components were the governing factors. Matsuura et al.[60,61] regarded the pervaporation mechanism as a combination of reverse osmosis (RO) separation,

followed by evaporation and vapor transport through the capillary pores on the surface layer of a RO membrane. Yoshikawa et al.[62-66] explained that specific and selective separation of substances through membranes may be realized by differences in strength of the hydrogen bonding interaction which leads to selective separation through the membrane. Raghunath and Hwang[67] suggested that in the pervaporation of dilute volatile organics, the liquid phase boundary resistance contributes significantly to the overall transport resistance and in many cases may overwhelm the membrane resistance.

With the occurrence of composite membranes, consisting of a dense top layer and of a porous substrate, a resistance model which is an analog of the Wheatstone bridge of an electric circuit has been developed by Henis and Tripodi.[68-70] A new resistance model for the transport of gases through laminated PDMS/PEI composite membranes was proposed by Matsuura et al..[71] They considered the resistance model proposed by Henis and Tripodi as a special case of new resistance model, where the resistance of the cross-flow between vertical parallel flows is set equal to zero. However, these models were only used for describing gas transport through the polymeric composite membrane. They are not to interpret the transport through the composite membrane in which particles are introduced into a polymer to form a membrane. Recently, te Hennepe et al.[34] have developed a resistance model to describe the pervaporation flux and selectivity for the separation of ethanol/water mixtures with silicate filled silicone rubber membrane. The model interprets the increased component flux for ethanol in terms of an increasing ethanol permeability for the membrane. Membrane permeability is given as a function of rubber and silicalite permeability and of the silicalite content of the membrane. This case is very similar to our research described in this

thesis. In this study, however, our interpretations are mainly based on the structure and properties of organo-clays used in the research, we are also interested in introducing this model into our research. A detailed description of this model will be given in Section 2.5.

2.4 Membranes for the pervaporation processes

The membrane governs the pervaporation process. In a pervaporation process, a significant membrane should combine the characteristics of high permeation through the membrane with good selectivity. In order to obtain good permeation rates and a high degree of separation for a liquid mixture, it is essential to choose the right membrane as well as the optimum operating conditions. Pervaporation was not employed on an industrial scale until quite recently. Apart from the fact that it was as energy intensive process, the main drawback was the unsatisfactory performance of commercial films and membranes.

Currently, the industrial applications of pervaporation are the dehydration of alcohols and of other organic solvents using hydrophilic or charged polymeric membranes, and the removal of small quantities of volatile organic solutes from water using hydrophobic membranes. Polymer membranes used in pervaporation can be of two kinds: glassy or rubbery (elastomers). This distinction is made on the ground of the state of the polymer at room temperature. Polymers with a glass transition temperature below room temperature are in the rubbery state at room temperature and are therefore classified as rubbery or elastomers. Polymers which have a glass transition temperature above room temperature are classified as glassy polymers. Generally, glass polymers permeate preferentially water.

Elastomers have a glass transition temperature below room temperature or working

temperature and most of the elastomers need to be crosslinked (or vulcanized) to obtain sufficient mechanical strength. The polymer chain of the elastomers contains rather small side groups which are non-polar. This results in a flexible structure which preferentially permeates organic substances and relatively high permeability. Membrane materials which are suitable for the selective removal of organics from water are therefore elastomers.

One of the most common elastomers is polydimethylsiloxane (PDMS). PDMS membranes have rather high organic fluxes. The water fluxes are, however, also quite high which results in high overall fluxes and reasonable selectivities.[72] The crosslinked PDMS membranes seem to have the greatest potential in pervaporation.[100,101] The reasons for this fact has been explained already qualitatively with a solution-diffusion model.[102,103] The relatively simple manufacture of the PDMS membranes and the high permeability for organic components resulted in an increase in research on vapour recovery and treatment of aqueous solutions using this membrane.[71,104]

For a membrane process, diffusion rates of penetrant in polymers generally depend on the mobility of the segments in the polymer chain. The chain flexibility in PDMS is determined by the presence of steric groups, by chain interactions and by the polymer backbone structure. Si-O bonds are well known for their high flexibility, whereas aromatic or heterocyclic groups in the chain and unsaturated bonds with trans configurations diminish the chain mobility. Side groups determine to a large extent chain interactions and affect the rotation of the main chain. Like in almost every elastomeric polymer, hydrogen atoms are the main substituent of the PDMS backbone. Because of the small dimensions of hydrogen atoms, the hydrocarbons have a relatively high mobility and high packing density. Both chain

mobility and chain interactions are altered when H-atoms are substituted by other atoms or groups.

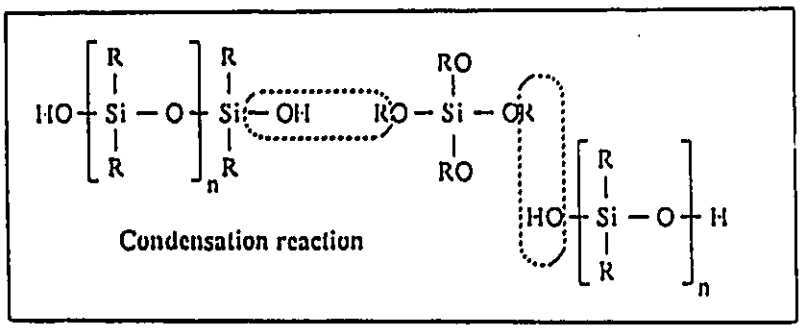

Figure 2.2 PDMS room temperature vulcanizing (RTV) system

Physical chain interactions can be subdivided into dipole forces, dispersion forces and hydrogen bonding forces. However, those interactions are relatively small compared to the chemical bonding of individual chains in macromolecules by crosslinking reaction. The terms cross-linking or vulcanization are both used synonymously for chemically bonding independent molecular chains into a molecular network. As a result of this vulcanization process, a rubber is obtained with improved mechanical and chemical properties. As a matter of fact, PDMS used as membrane material is usually cross-linked. It can be cross-linked by a room temperature vulcanization (RTV) reaction. In this system, cross-linking occurs either through a catalyzed hydroxy condensation, as indicated in Figure 2.2.

In the condensation reaction, a hydroxyl end-blocked polysiloxane is mixed with a polyfunctional organosilicate that act as a cross-linking agent and with a catalyst to promote condensation. This reaction takes place already at room temperature. In this system, the cross-linking agent becomes a part of the network, but, because it is also a silicone, the heat stability is not altered. In RTV-systems, the condensation reaction is commonly applied.

Many studies in pervaporation using PDMS membranes can be found in literature. Table 2.1 gives a summary of organic enrichment by pervaporation through PDMS membrane[52].

Table 2.1 Organic enrichment by pervaporation through PDMS as record by mass spectrometry

Organic compounds	Separation factor (α)
Acetic acid	3
Ethanol	7
Acetaldehyde	48
Acetone	50
Pyridine	70
n-Hexane	1300
Ethyl ether	1600
n-Butyl acetate	2300
1,2-Dichloroethane	4300
Chloroform	6800
Vinyl chloride	9000
Cyclohexane	9300
Toluene	10000
Benzene	11000
Styrene	13000

In order to test the hypothesis that organo-clay can be used as membrane materials

for continuous separation processes, pioneer work has been carried out by H. Lao[12] in gas separation in our laboratories. In his studies, the maximum pure gas permeability ratios achieved for CO_2/CH_4 and O_2/N_2 were 8.7 and 4.1 in TAA1-M-PDMS-45 and MMDA-M-PDMS-45 membranes as compared to 3.9 and 2.3 which were obtained for organo-clay free PDMS membranes. Some preliminary results of pervaporation have also been obtained with organo-clay-PDMS membrane[12]. From the previous results in our laboratories, it was found that the organo-clay-PDMS composite membrane was water selective in pervaporation process, when using ethanol/water mixture as a feed solution. In other words, when organo-clay is added to PDMS, the membrane is changed from organic component selective to water selective. It is obvious that further investigations into these type of membranes are of great interest.

In the present work, PDMS membranes were filled with various organo-clay materials, serving as sorptive fillers. The organo-clay materials were made by exchanging the interlayer cations of montmorillonite (M) with organic cations such as tetraalkylammonium (TAAn) or tetraphenylphosphonium (TPP). Organo-clay-PDMS membranes were prepared and tested to further investigate the performance of these membranes in the pervaporation process.

In order to improve the separation characteristics of the PDMS membranes, different modified PDMS membranes have been studied intensively. It was found that a decrease of the PDMS membrane thickness can effectively increase the flux with only a small cost of selectivity. Based on this study, a composite membrane which consists of a very thin and dense PDMS top layer and a substrate was developed. In this type of membrane, the

selectivity and the flux both depend on the top layer. Then, the use of fillers to form different type of composite membrane has been recommended.[34,73] In the very beginning, the idea of adding filler, such as silica, into PDMS was for improving the mechanical strength.[74] The development of zeolite filled PDMS membranes has focused on a renewed interest on the improvement of the performance of these membranes by incorporating highly selective zeolite molecular sieves into polymer membranes.[34,35] The pore size and the structure of a silicone-rich zeolite has an effect on the sorption behaviour. The aluminium content of zeolite can be varied by several orders of magnitude. This fact is responsible for the hydrophobic character of the zeolite causing hydrophobic molecules to be adsorbed preferentially.[75] Silicalite-1, synthesized for the first time in 1977,[76] is a crystalline silica molecular sieve. Unlike aluminosilicate zeolite which are hydrophilic, silicalite is hydrophobic and capable of selectively adsorbing organic molecules from aqueous solution. According to the results of te Hennepe et al.,[34,35] their silicone rubber membrane filled with silicalite-1 shows a much improved selectivity and flux in pervaporation for removing alcohols from aqueous solutions. The selectivity α of ethanol over water for their membrane rises from 7 to as high as about 40, when the silicalite content increases from 0 to 70 wt%. The flux also rises from 0,02 to 0,045 l/m^2 h, implying a facilitated transport of ethanol molecules through the silicalite. The results of Meng-Dong Jia et al.[77] illustrated that by application of self-synthesized ultrafine silicalite crystallites (0.2-0.5μm) and prepolymerization of the suspension consisting of silicalite, PDMS and isooctane, thin film composite membranes could be prepared. Active layers of the composite membranes as thin as 3μm were achieved, resulting in a high flux. Silicalite to PDMS ratios (w_s/w_p) in the active layer were increased to 3.3, resulting in

selectivities as high as 34 for separating ethanol from water.

Recently, Lao[12] has reported a study on gas separation of PDMS membranes filled with different organo-clay materials, consisting of PDMS and TAAn-M or TPP-M. The maximum pure gas permeability ratios achieved for CO_2/CH_4 and O_2/N_2 were 8.7 and 4.1 in TMA-M-PDMS-45 and MMDA-M-PDMS-45 membranes as compared to 3.9 and 2.3 which were obtained for organo-clay free PDMS membranes. With a zeolite filled PDMS membrane of 18μm thickness and a silicalite to PDMS weight ratio w_s/w_p of 1.6, an O_2 and N_2 selectivity of 2.7 were reached.[77] Some preliminary results of pervaporation were also obtained with organo-clay-PDMS membrane.[12] From the previous results, it was found that the organo-clay-PDMS composite membrane was water selective in pervaporation process, when using ethanol/water mixture as a feed solution. In other words, when organo-clay was added to PDMS, the membrane changed from organic component selective to water selective.

In this research, organo-clay-PDMS membranes were prepared and tested to further investigate the performance of these membranes in pervaporation processes.

2.5 Resistance model through organo-clay-PDMS composite membrane

As described above, a number of transport models for pervaporation process can be found in literature. In this study, a composite membrane is formed by introducing organo-clay particles into the PDMS polymer matrix. In this case, the addition of organo-clay particles to the PDMS membrane influences both the sorption part and diffusional part of the sorption-diffusion model which is frequently used to describe the transport through

pervaporation membranes[32,33]. A resistance model has been recently developed by te Hennepe et al.[35] to describe the transport through particle-filled composite membranes. This model draws an analogy between the behaviour of particle filled polymeric composite membrane for pervaporation and current flow through an electrical circuit. A critical factor in the behaviour of such composite membrane is that each of the components is located in well-defined domains which in turn may have a different resistance to transport. In the resistance model, diffusion through the membrane is considered to be rate determining[105]. With this resistance model, the flux through particle-filled composite membrane can be described. Based on this model, a modified resistance model was developed by Lao[12] for gas separation using organo-clay filled PDMS composite membranes. In this modified model, the effect of microporosity of organo-clay on the resistance of the membrane was taken in account. With combining those two models, a new resistance model can be established for description of transport through the organo-clay filled PDMS composite membrane in pervaporation.

The permeation rate, or flux, for component i through a polymeric membrane can be described by:

$$J_i = P_i A \Delta p_i / l \qquad (2\text{-}3)$$

where J_i is the permeation rate of component i, P_i is the intrinsic permeability of the polymeric membrane to component i, A is the cross sectional surface area of the membrane available for permeation, l is the thickness of the membrane through which the component permeates, and Δp_i is the partial pressure difference.

Using the electrical analog, the above relationship describing permeation through a polymer membrane is mathematically equivalent to Ohm's law which describes current flow through a resistor:

$$I = E/R \tag{2-4}$$

Conceptually, the current, I, can be equated with the permeation rate, J. The driving force for current flow, (i.e. the difference in electric potential E), is analogous to the concentration (partial vapour pressure) gradient Δp_i. We can define, then, a resistance to permeate flow, R_i, which is equivalent to the electrical resistance R:

$$R_i = l/P_iA \tag{2-5}$$

so that combining (2-3) and (2-5), a basic equation of resistance model can be obtained:

$$J_i = \Delta p_i/R_i \tag{2-6}$$

This equation shows that J is a function of the difference in partial vapour pressure and the resistance of the membrane. The main objective is to find an expression for R for feed component i. Since transport can occur through both PDMS and the organo-clay particles, membrane resistance R_i can be written as a combination of the resistances for both materials:

$$R_i = R_{1,i} + R_{3,i} \qquad (2\text{-}7)$$

Where $R_{1,i}$ is the resistance of PDMS for the component i and $R_{3,i}$ the resistance of the organo-clay for the component i. In equation (2-7), the total resistance through the membrane seems to be considered as $R_{1,i}$ and $R_{3,i}$ in series. However, if the organo-clay particles are impermeable, there is still the transport route around the particles, and this effect has to be considered as a third resistance, $R_{2,i}$ which is parallel to the organo-clay resistance $R_{3,i}$ in equation (2-7).

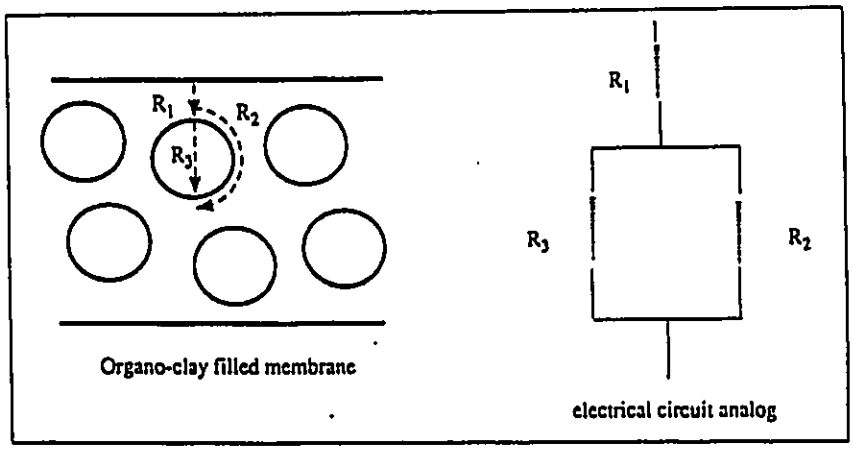

Figure 2.3 **Schematic representation of the organo-clay filled PDMS membrane and its electric circuit analogue**

Figure 2.3 gives a schematic representation of the resistance model which describes the transport through organo-clay-PDMS membranes. The membrane resistance is a combination

of resistances in series and in parallel, as in a electrical circuit analogue. The total membrane resistance can be written as :

$$R_t = nR_{1,t} + [nR_{2,t}R_{3,t} / (R_{2,t} + R_{3,t})] \quad (2\text{-}8)$$

Where n is the number of organo-clay particles along the transport path. The individual resistances in equation (2-8) can be determined in term of permeabilities as given in equation (2-9a) to (2-9c):

$$R_{1,t} = R_{PDMS,t} = l_1/P_{1,t}A_0 \quad (2\text{-}9a)$$

$$R_{2,t} = R'_{PDMS,t} = l_2/P_{2,t}A_p \quad (2\text{-}9b)$$

$$R_{3,t} = R_{Organo\text{-}clay,t} = l_3/P_{3,t}A_c \quad (2\text{-}9c)$$

In the above relations, l_1 is the pathlength between the successive clay particles in the direction of transport. l_2 is the length through the PDMS around the organo-clay particles, and l_3 is the length of organo-clay particles. A_0 is the total membrane area, A_p is the area between the clay particles and A_c is the area perpendicular to the flow as occupied by the clay in a cross section. The total thickness can be described as:

$$nl_1 + nl_3 = l \quad (2\text{-}10)$$

The pathlength around the organo-clay particles is a function of the organo-clay particle size, particle geometry and particle orientation. Here, we assume that the organo-

clay-PDMS particles are homogeneous and spherical. For spherical particles oriented as shown in Figure 2.4. Equation (2-11) gives a simple relation between l_2 and l_3 :

$$l_2 = \pi/2 l_3 \qquad (2\text{-}11)$$

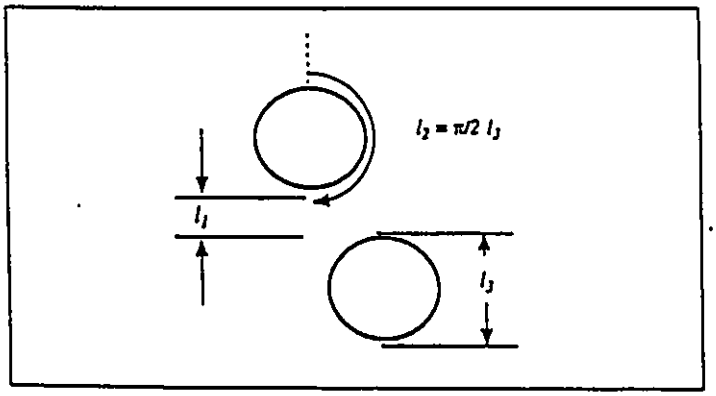

Figure 2.4 Schematic representation of organo-clay particles in the PDMS composite membrane and pathlengths through and around the particles

According to Nielsen[106], who described the flux through a polymer membrane filled with inert particles, the space between the particles in the direction of transport is related to the polymer content of the membrane ϕ_p (= 1-ϕ_c, ϕ_c is the filler content in the membrane).

The factor n, the number of layers, can thus be eliminated. Combination of equation (2-11) with equation (2-10) leads to the relations (2-12a) and (2-12b). These equations give the pathlength through the polymer part and through the organo-clay part of the membrane, respectively.

$$nl_1 = (1-\phi_c^{1/3})l \qquad (2\text{-}12a)$$

$$nl_3 = \phi_c^{1/3} l \qquad (2\text{-}12b)$$

where ϕ_c is the organo-clay content in the composite membrane. Further, the expressions for the area of the polymer between the particles and the particle area in a cross section can be written by:

$$A_p = A_0\,(1-\phi_c) \qquad (2\text{-}13a)$$

$$A_c = A_0\phi_c \qquad (2\text{-}13b)$$

By combining the above equations, the individual resistances and the total resistance, (R_t), across an organo-clay-PDMS membrane can be expressed as:

$$(R_1)_i = nR_{1,i} = (1-\phi_c^{1/3})l/P_{PDMS,i}A_0 \qquad (2\text{-}14a)$$

$$(R_2)_i = nR_{2,i} = \pi/2\phi_c^{1/3} l/P_{PDMS,i}(1-\phi_c)A_0 \qquad (2\text{-}14b)$$

$$(R_3)_i = nR_{3,i} = \phi_c^{1/3} l/P_{Organo\text{-}clay,i}\phi_c A_0 \qquad (2\text{-}14c)$$

$$(R_i)_l = (1/A_0)[(1-\phi_c^{1/3})l/P_{PDMS,i} + \pi/2\phi_c^{1/3}l/(P_{PDMS,i}(1-\phi_c) + \pi/2P_{organo\text{-}clay,i}\phi_c)]$$

(2-15)

Therefore, the component flux is given as a function of the organo-clay content of the membrane, of the membrane thickness, of the membrane area and of the permeabilities of the membrane constituents:

$$J_i = \Delta p_i A_0/[(1-\phi_c^{1/3})l)/P_{PDMS,i} + \pi/2\phi_c^{1/3}l/(P_{PDMS,i}(1-\phi_c) + \pi/2\ P_{Organo\text{-}clay,i}\phi_c)]$$

(2-16)

From equation (2-3) and (2-16), the total permeability of organo-clay PDMS composite membrane can be obtained.

$$(P_i)_l = l/[(1-\phi_c^{1/3})l)/P_{PDMS,i} + \pi/2\phi_c^{1/3}l/(P_{PDMS,i}(1-\phi_c) + \pi/2\ P_{Organo\text{-}clay,i}\phi_c)]$$

(2-17)

The permeability for polymer matrix $P_{PDMS,i}$ and organo-clay $P_{organo\text{-}clay,i}$ can be calculated by fitting the equation (2-17) on permeation data. It is reasonable to assume that both PDMS and organo-clay permeabilities are independent of the organo-clay content of the membrane. Also both permeabilities are average values which can be measured only for the membranes as a whole. Both permeabilities may vary with the position of the particles inside the membrane. The model does not account for these variations.

Regarding the overall resistance $(R_i)_l$, there are three resistance contributions, $(R_1)_l$, $(R_2)_l$, and $(R_3)_l$, respectively. In the case of a composite membrane which contains impermeable particles, the overall resistance has only two components $(R_1)_l$ and $(R_2)_l$, since

$(R_3)_l$ is infinity. Therefore equation (5-15) becomes

$$(Rt)_l = (R_1)_l + (R_2)_l = nR_{1,l} + nR_{2,l} \qquad (2\text{-}18)$$

In the case of a composite membrane containing lower organo-clay content and medium microporosity in the organo-clay particles, the overall resistance is governed by three components $(R_1)_l$, $(R_2)_l$, and $(R_3)_l$. As the content and the microporosity of the organo-clay in the composite membrane increase, the resistance component through the organo-clay particles $(R_2)_l$ becomes smaller and the most of permeant transports through the $(R_3)_l$ side. As a result, the overall resistance through the highly microporous organo-clay-PDMS composite membrane is governed by $(R_1)_l$ and $(R_3)_l$. Therefore the permeability of the organo-clay PDMS composite membrane is a function of organo-clay content and the microporosity of the organo-clay.

2.6 Characterization of pervaporation membranes

The characterization of pervaporation membranes can be broadly classified in the following categories:[78]

· Physical and chemical properties of the polymer. The interaction between the polymer and the penetrants. For example, glass transition temperature and degree of crystallinity of the polymer.

· Surface analysis or morphology of the membrane. The morphology of the membrane is generally characterized by the pore size and the pore size distribution on the

active surface layer of the membrane.

· Permeation rate and selectivity of the membrane under pervaporation conditions. The most effective and the simplest method for the characterization of a pervaporation membrane is by measuring the permeation rate and the selectivity under actual pervaporation conditions. Since the permeate undergoes a phase change during the pervaporation, mass fluxes are most commonly considered. The permeation rate is usually defined as mass (or moles) permeation through 1 m^2 of the membrane per unit time (mole/m^2·h or g/m^2·h).

With respect to selectivity, two different parameters α and β can be alternatively used. The separation factor, α, is defined as:

$$\alpha = [X_p(1-X_f)]/[X_f/(1-X_p)] \qquad (2\text{-}19)$$

Here X_f and X_p refer to the mole fractions of a component in the feed mixture (upstream) and in the permeate stream (downstream), respectively. The separation factor, α, is patterned after the relative volatility of the components of binary liquid mixtures. The α parameter is independent of concentration units used.

The selectivity (enrichment factor) of a membrane can also be expressed by the β parameter. This parameter is defined as:

$$\beta = X_p/X_f \qquad (2\text{-}20)$$

The enrichment factor β is simply the ratio of the concentrations of the preferentially

permeating species in downstream and upstream.

Sometimes, the overall performance of the membrane is evaluated by the parametric values of J and α, where J is the permeation rate and α is selectivity. The value of J and α was named as pervaporation separation index (PSI) by Huang and Yeom.[79] This index is a relative measurement of the separation ability of a membrane. This index also can be used as a relative guideline for the design of pervaporation membrane separation processes and to select a membrane with an optimum combination of permeation rate and selectivity. It is clear that α is systematically larger than β since α and β can be interconverted by using the following relationships:

$$\alpha = (1-X_p)\beta/(1-\beta X_p) \qquad (2\text{-}21)$$

β is very convenient way to formulate the chemical engineering equations governing a continuous pervaporative fractionation. On the other hand, α is more significant from the physico-chemical point of view, since it assumes an infinite value when the investigated membrane is perfectly semi-permeable $(X_p=1)$.

Chapter 3

Experimental

3.1 Purification of Montmorillonite

3.1.1 Purification of Montmorillonite[3,12]

A suspension of 15g of the crude montmorillonite (SWy-1) in 200 ml of water was prepared. Then, 1N HCl was added until the pH reached 3.5 and remained at or near this value for 10 minutes to destroy the carbonates. The mixture was centrifuged, the clear supernatant discarded and the sediment washed with HCl (pH 3.5) to remove soluble salts and exchangeable basic cations. After a second centrifugation, the sediment was redispersed in 200 ml of water, the pH of the suspension was adjusted to 8.0 with 0.1N NaOH and the suspension was covered and allowed to stand overnight. It was then transferred to a 600 ml beaker marked 10 cm from the inside bottom. Water was added to the mark. The suspension was sonified for 15 minutes and it was then stirred overnight.

The $<0.2\mu m$ fraction of the clay was then separated by gravitation. After standing undisturbed and free from vibrations overnight, the suspension above the sediment was

siphoned off and poured into a large vessel. Water was added to the sediment up to the mark and the sediment was redispersed. The suspension temperature was taken and it was allowed to stand for the length of time needed for all particles larger than 0.2μm to deposit at the bottom of the beaker (6 hours in our case). The suspension above the sediment was then siphoned off and combined with the one siphoned off previously. This was repeated until the supernatant liquid became clear after the 6 hours waiting period. The siphoned suspension that contained all the $<0.2\mu$m clay was sonified for 15 minutes and then acidified to pH 3.5 with 1N HCl, Furthermore, 75 ml of a saturated NaCl solution was added to prepare the homoionic $< 0.2\mu$m Na^+-montmorillonite. This caused the flocculation of the suspension. Most of the clear supernatant could then be siphoned off and discarded. The suspension was transferred into a dialysis tubing and it was placed in a large bath with deionized water (dialysis: membranes spectrapor, molecular weight cutoff=3500). The water was replaced regularly until a negative Cl^- ion test in the suspension was achieved. It took at least 1 week. The sediment was then freeze-dried for 3 days.

3.1.2 Particle size analysis

The $<0.2\ \mu$m fraction of the homoionic Na^+-montmorillonite was checked by particle size analysis using a Sedigraph 5100 instrument. 2% suspension solution of the clay (2g/50ml of sodium metaphosphate 0.5%, temperature 34.5 $^\circ$C) was prepared and then transferred into a cell. The density of montmorillonite (2.54 g/cm^3) used in this research is a theoretical value.

3.2 Preparation of Organo-clays

Tetraalkylammonium (TAAn) and tetraphenylphosphonium (TPP) ions were chosen as organic cations to make the organo-clay. All the chemicals were obtained from Aldrich Chemical Co., and used without further purification. The tetraalkylammonium (TAAn) and tetraphenylphosphonium (TPP) cations were incorporated into the interlamellar spaces of Na-montmorillonite at full cations exchange capacity (CEC; 87±5 mequiv./100g of clay). The tetraalkylammonium bromide or iodide and tetraphenylphosphonium bromide were dissolved in distilled water or 20%-70% of methanol/water mixtures before 100g of clay was added into the solution. The mixture was stirred overnight for complete exchange and the mixture was filtered and washed with distilled water or methanol/water mixture until it became bromide or iodide free. The resulting organo-clay was then dried under vacuum at 60 °C overnight. Organo-clay particles smaller than 63 μm were collected by sieving for membrane preparation.

3.3 Preparation of Membranes

3.3.1 Preparation of PDMS membranes

The PDMS membranes were prepared from RTV615A and RTV615B (curing agent) which were obtained from General Electric Company without further purification. The RTV615A and RTV615B were mixed in 10:1 ratio. After stirring for 2 hours, the mixture resulted in a paste which was cast on a glass plate to the thickness of 8 mil. The film was cured on the glass plate at 70 °C for 16 hours.

3.3.2 Preparation of organo-clay-PDMS composite membranes

The organo-clay-PDMS membranes were prepared by mixing a PDMS solution (RTA615A and RTV615B in 10:1 ratio) with appropriate amount of organo-clay to form a paste. Then, the paste was cast on a glass plate to form a film. The film was cured on the plate at 70 °C for 16 hours. In the case of the preparation of organo-clay-PDMS membranes in which the content of organo-clay was 40% and 50%, 1.5 ml and 2.5 ml of hexanes were added into the mixture of organo-clay and PDMS polymer in order to make a polymer solution. The membranes with 60% and 70% organo-clay were not obtained because they were too fragile.

3.3.3. Measurement of membrane thickness

The thickness of the membranes was measured by a micrometer after curing. It was in the range 85-110 μm. The organo-clay content and the resultant membrane thickness for the membranes used in this study are listed in Table 3.1.

Table 3.1 Membrane composition and thickness

Membrane	Organo-Clay Content (wt%)	Membrane Thickness (μm)
Pure PDMS-1		52
Pure PDMS-2		107
Pure-M	40	92
TAA1-M-PDMS	20	114
	30	102
	40-1	134
	40-2	96
TPP-M-PDMS	20	92
	30	102
	40-1	96
	40-2	88
	47	110
Pure PDMS-3		103
TAA3-M-PDMS	50	83
TAA4-M-PDMS	50	93
TAA5-M-PDMS	50	85
TAA6-M-PDMS	50	95
TAA7-M-PDMS	50	95
TAA6-M-PDMS	20	112
	30	94
	40	104
	50	95

3.4 Methods for characterizing organo-clays and organo-clay-PDMS membranes

3.4.1 Powder X-ray diffraction spectrum

3.4.1.1 Preparation of samples

The unoriented samples for X-ray analysis were prepared by smearing a thin layer of vaseline on a low background holder and then the holder was uniformly covered by Na^+-montmorillonite or organo-montmorillonite powder.

The oriented Na^+-montmorillonite sample for X-ray analysis was prepared by dispersing about 20 mg of sample in distilled water and allowing to dry in air.

For X-ray analysis of organo-clay-PDMS membrane, the membrane was pasted on the holder with a scotch tape.

3.4.1.2 X-ray diffraction spectrum

The samples were recorded in a PHILIPS PW 3710 X-Ray diffractometer using Cu kα X-radiation at University of Ottawa. The X-ray diffraction patterns for different organo-clays were examined in order to determine the interlayer spacing of the clay and organo-clays. This method was also used for monitoring structural changes of the organo-clay in the membrane resulting from the pervaporation process.

3.4.2 Measurement of surface area

The Brunauer-Emmet-Teller (BET) gas adsorption method has become the most

widely used standard procedure for the determination of the surface area of finely divided and porous materials.

The N_2 adsorption measurements were performed in ASAP 2000 analyzer in the Chemical Engineering Department, University of Ottawa. The instrument introduced the adsorbate gas continuously to the sample through a mass flow controller. The temperature of the sample is maintained at liquid nitrogen temperatures (77K) and the rate of gas flow was maintained constant throughout the process. For the measurement of nitrogen adsorption isotherms, the samples were dried in an oven at 120-140°C overnight under vacuum. The samples were outgassed for 3 hours at 150°C at 10^{-4} - 10^{-5} torr. A dewar flask containing liquid nitrogen was placed around the sample tube and the level of nitrogen was kept by periodically replacing the liquid lost by evaporation.

3.4.3 Thermogravimetric analysis (TGA)

Thermogravmetric analysis was carried out on thermal stability of organo-clays and organo-clay-PDMS membranes on a polymer Labs STA 1500H model thermogravimeter with alumina reference and sample pans under flowing nitrogen (40 cc/min) to remove any decomposition products. The crucible was lowed into the furnace and heating rate ranging set at 20 °C per minute to about 1200°C. Organo-clays were heated at 220°C in furnace for 3 hours before taking the measurement of TGA. The membranes were measured without any pre-heating treatment.

3.5. Experimental apparatus for pervaporation process

3.5.1 System 1

This equipment was set up at Department of Chemistry, University of Ottawa. A schematic diagram of the apparatus is shown in Figure 3.1. The cell for the pervaporation experiments was the same as the static cell used in reverse osmosis and ultrafiltration experiments. For flux determination, the effective area of membrane was 10.2 cm^2. About 80 ml of feed liquid was loaded in the permeation cell. Vacuum was generated at the downstream side of the membrane, while the upstream pressure was maintained at an atmospheric pressure. The permeate sample was condensed and collected in a cold trap with liquid nitrogen. The permeation flux was determined by measuring the weight of the sample collected during a predetermined period. The downstream was controlled below 2 mbar.

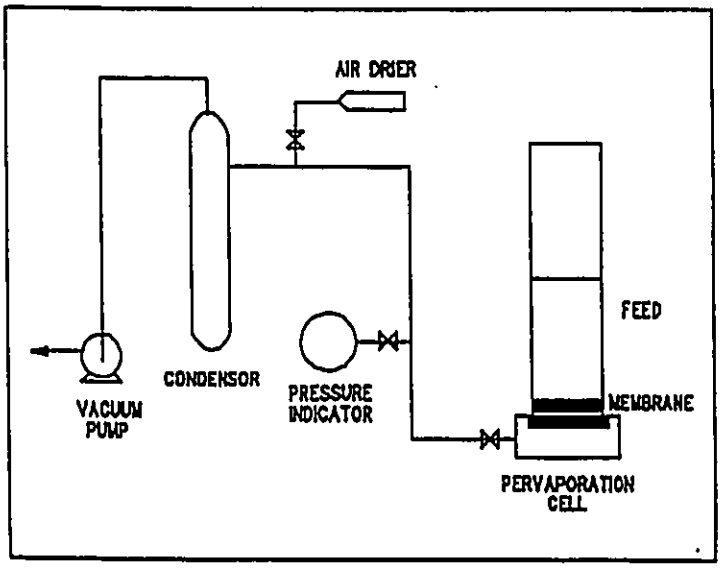

Figure 3.1 Schematic diagram of pervaporation apparatus

3.5.2 System 2[96]

Pervaporation equipment at the Chemical Engineering Department of McMaster University is a novel automated pervaporation testing apparatus which allows for on-line data acquisition. Figure 3.2 shows a schematic of the pervaporation testing apparatus. The cells are made of stainless steel and are configured for radial flow of the feed solution across the membrane surface. The effective membrane surface area is 32.6 cm^2. Viton O-ring seals the liquid and vapor sides of the membrane ensuring that there is no surface or cross sectional leaking of the permeate or feed streams. The permeate chamber in the cell contains a thermocouple for measurement of permeate vapor temperature. The cell has a port on the permeate side for sweep gas applications. The vacuum pressure at the permeate side of the membrane is measured by the pressure transducer and controlled by a control valve. The permeate flow rate is measured by a mass flow meter. Each cell has two solenoid ON/OFF valves in order to divert the permeate flow from the particular cell either to the cold trap or to the 10 ml injection loop for analysis by gas chromatography (GC). This configuration allows for the remaining cells to be operational while one membrane is analyzed by GC.

Accurate determination of the permeate composition is achieved by measuring the temperature and pressure with a thermal couple and pressure transducer, respectively, of the vapor permeate by 10 ml injection loop at the GC instrument. The injection of sample onto the column is performed automatically by pneumatic actuated Valco valves. The feed solution composition is then evaluated. A Valco valve having 1 ml internal injection loop places the sample onto a second column.

A centrifugal pump circulates the feed solution from the 10 L feed tank to the cells,

along the feed line. The cells are connected in series with respect to the feed solution. The feed tank volume should prevent a significant change in the feed solution composition to occur over a testing period. The feed tank lid is fitted with a condenser. A 5 psig maximum nitrogen gas blanket can be placed in the head space of the feed tank to prevent volatile

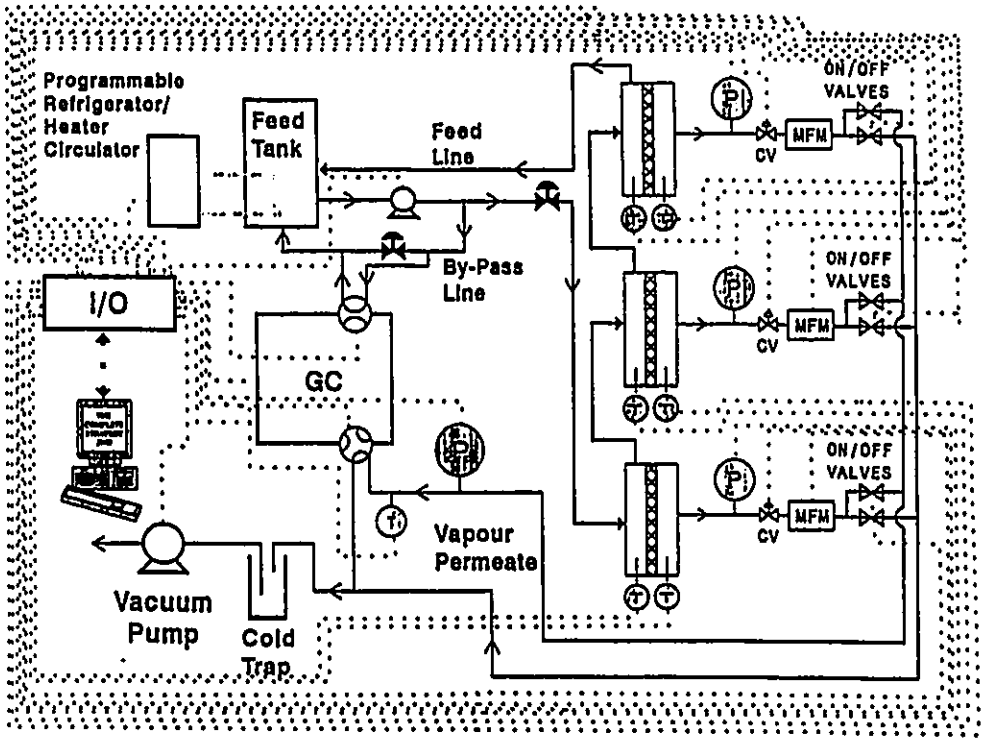

Figure 3.2 **Schematic of pervaporation testing apparatus, (CV) control valve, (GC) gas chromatography, (I/o) Tansduction box, (MFM) mass flow meter, (p) pressure transducer, (T) thermocouple, (--) data communication.**

component evaporation. Manual adjustment of feed valve regulates the feed solution flow rate to the cell. The by-pass valve regulates the flow in the by-pass line and to the 1 ml internal injection loop. Agitation of the feed solution in the feed tank is provided by the by-pass line. The volume of liquid in the feed side of the all cells and lines from the cells to the feed tank can be displaced by nitrogen gas so the operator is not exposed to hazardous substances when change membranes.

The programmable refrigerator/heater circulator monitors the feed solution temperature in the feed tank by a thermocouple. The Complete Strategy (a process control software) monitors the feed solution and permeate vapor temperature by a thermocouple at the feed and permeate chamber, respectively, of each cell.

3.6 Preparation of feed mixture solutions

3.6.1 1,2-dichloroethane/water mixture solution

The 1,2-dichloroethane (DCE) used in the experiment was from Fisher Scientific Inc. without further purification. An appropriate amount of DCE was directly added into the 8 L. tank filled with distilled water. The concentration of DCE in the tank was kept at about 60-70 ppm. During the experiment, a calculated amount of pure DCE solution was added into the tank, when GC result shows that the concentration of DCE was below 60 ppm.

3.6.2 Benzene/water mixture solution

The benzene used in System 1 was from BDH Chemicals without further purification.

A calculated amount of benzene was added into 500 ml distilled water to give a 250-350 ppm benzene solution. The concentration of benzene in the solution was monitored by GC.

3.7 Gas chromatography experiments

Gas chromatography were used for analyzing the concentration of organic components in feed and permeate during the pervaporation experiments.

3.7.1 GC experiments in system 1

3.7.1.1 Preparation of GC samples

Benzene/water mixture was used as feed solution in System 1. The concentration of benzene in the feed was measured by directly injecting the feed sample into the GC.

The permeate was a concentrated benzene/water mixture solution. This solution was diluted with appropriate volume of water before injecting into the GC.

3.7.1.2 Conditions of the gas chromatography

A GOW-MAC 69-550P model gas chromatography with a thermal conductivity detector and a SP4270 chromatography integrator was used in System 1. A stainless steel column of 6 feet length and 1/8 inch outer diameter packed with GAS CHROM 254 was used for the analysis of benzene concentration in water. The velocity of helium carrier gas was 40 ml/min. The column temperature was initially controlled at 100°C and a temperature program allowed temperature increase to 200°C in 10 min. The injector temperature and the

detector temperature were 220°C and 200°C respectively.

3.7.2 GC experiment in system 2^{96}

3.7.2.1 Conditions of GC

A HP5890A model gas chromatography with FID detectors was directly connected with the outlet of permeate before the vacuum pump. A process control software package GENESIS referred to as the Complete Strategy, by Iconics Inc., provides algorithms for real-time data acquisition and supervisory control. The Complete Strategy contains C-code routines developed for communication and data transfer with the HP3392A integrator. Conversations between the Complete Strategy and GC occurs through the HP3392A integrator. The Complete Strategy provides the GC with the detector conditions prior to injection, and the peak analysis performed by the integrator is transmitted to the Complete Strategy for storage to disk.

The column was packed with PROPOC. Two FID detectors were mounted in the GC for analyzing the feed and the permeate respectively. During the membrane test, the feed solution and the permeate were directly injected into the GC by relay control valve. At the same time, temperature and pressure at the GC were recorded and the concentration of the feed and permeate were calculated.

3.8 UV spectroscopy experiment

A Gilford (Response) UV spectroscopy was employed for analysis of concentration

of benzene in feed and permeate. The wavelength used was 254 nm. Distilled water was used as reference. A standard curve was prepared by measuring freshly prepared samples containing different concentration of benzene and the absorbance value versus the concentration of benzene was plotted. The maximum concentration of benzene in this curve was 500 ppm. The curve shows a linear relationship between the absorbance and the concentration of benzene. The feed solution was directly measured and the permeate was diluted to about 3 ml in order to fill up the cell.

This method was replaced by GC analysis later in order to improve the sensitivity.

Chapter 4

Characterization of organo-clays and of organo-clay-PDMS membranes

4.1 Introduction

The layered structure of montmorillonite was discussed in Chapter 1. Due to isomorphous substitution, montmorillonite carries a permanent negative charge in its structural framework. The negative charge of the clay layer is counterbalanced by sorption of an equivalent amount of extraneous inorganic cations such as sodium, calcium or potassium, and the inorganic cations in the clays can be replaced by organic cations.

It has been shown that when the natural interlamellar inorganic cations of montmorillonite were replaced by small alkylammonium organic cations, permanent microporosity could be created, and that sorption of gases and of organic molecules was then very favored.[80] An alkylammonium cation of larger size could cause the formation of a bilayer structure in the interlamellar space of montmorillonite. The characterization of organo-clays is presented and discussed in this chapter using XRD, BET and TGA.

In this research, the intercalation of tetraalkylammonium and tetraphenylphosphonium cations into montmorillonite has been studied. The alkylammonium cations are known to

cause considerable modifications in the hydration and swelling properties of montmorillonite.

4.2 Interlamellar spacing of organo-montmorillonite

X-ray diffraction is the most widely used technique for identification and characterization of clay minerals. This is especially true in the case of modified clay minerals, when the interlayer spacings are variable. Since montmorillonite is an expandable clay, the insertion of various cations between its layers may cause different interlayer spacings. The spacings in most organo-clays are in the range of 4-5 Å, which is larger than in the parent clays. The orientation of the cations in the interlayer spaces is strongly dependent on the size of the cations and on the charge density. For example, Na^+-montmorillonite has a spacing of 2.8 Å,[81] the insertion of various quaternary ammonium cations into Na^+-montmorillonite expands the interlayer spacing to 4 to 5 Å.[82-84] In the case of large molecules (with long carbon chains), the interlayer spacings could reach 9-10 Å. This was attributed to some overlap between the carbon chains. In this research, different types of organic cations, tetraphenylphosphonium and tetraalkylammonium, were intercalated into montmorillonite to form organo-clays. The change of the *d* spacing of the organo-clay was monitored by X-ray diffraction.

X-rays are electromagnetic radiations characterized by wavelengths between 0.1 and 4.5 Å. They are generated when electrons collide with the atoms of an obstacle. The energy lost by the electrons in these collisions is emitted as X-ray photons. The wavelengths of these photons are a function of the amount of energy lost by the electrons during the encounters. This gives rise to a continuous spectrum of X-ray radiation.[85] In the selection of a diffraction

beam, a monochromatic (single wavelength) X-ray beam simplifies the analysis of structural spacing in clay minerals.

X-ray diffraction can be conveniently visualized as a reflection of the incident beam by parallel, closely spaced planes of atoms within a crystal. The reflected rays combine to form a diffracted beam only if they differ in phase by whole number of wavelengths, that is, if the path length difference is equal to a multiple of the wavelength of the X-ray used. The condition for reflection is met only when the Bragg's equation is satisfied:[86]

$$n\lambda = 2\,d\,\sin\Theta \qquad (4\text{-}1)$$

where λ is the wavelength of the X-ray, d the spacing between the lattice planes and Θ the angle of incidence of the X-ray beam. Figure 4.1 shows a beam of parallel X-rays of wavelength λ falling at angle Θ onto the face of a crystal possessing a layer structure of parallel planes of atoms with spacing d.[87]

The X-ray spectrum of a layered clay composed of a series of equidistant peaks, can be obtained by varying Θ. A schematic representation of an X-ray spectrum of mica is shown in Figure 4.2. The first of these peaks corresponds to d, since $d = n\lambda/(2\sin\Theta)$ and $n=1$; the second peaks measures $d/2$, the third $d/3$ and so forth. Thus, the d value may be determined by averaging out these contributions for all of the visible peaks:

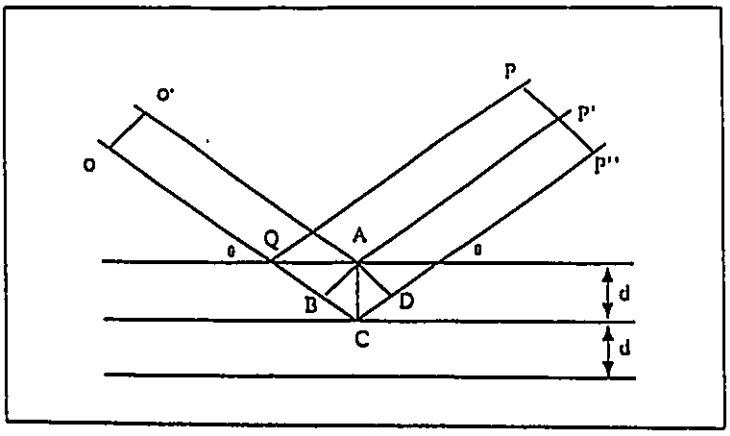

Figure 4.1 X-ray diffraction from a layered structure

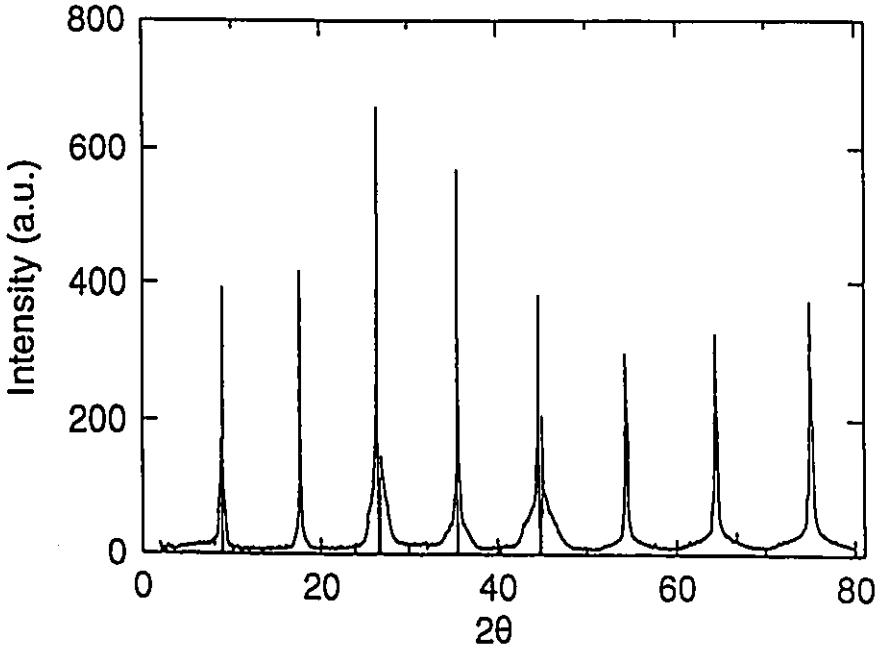

Figure 4.2 A schematic representation of an X-ray spectrum of mica

$$d_{av} = (d_1 + 2d_2 + 3d_3 + 4d_4 + \cdots + nd_n)/n \qquad (4\text{-}2)$$

$$n = 1, 2, 3, 4, \cdots$$

This calculated d value represents the distance from the middle of a clay layer to the middle of a subsequent clay layer. Therefore, the interlayer spacing d_{is} of the montmorillonite can be given by:

$$d_{is} = d_{av} - 9.6\,\text{Å} \qquad (4\text{-}3)$$

where 9.6 Å is the thickness of a layer of montmorillonite which is the distance between the two repeating layers without the interlayer cations. This is shown in Figure 4.3[86,88].

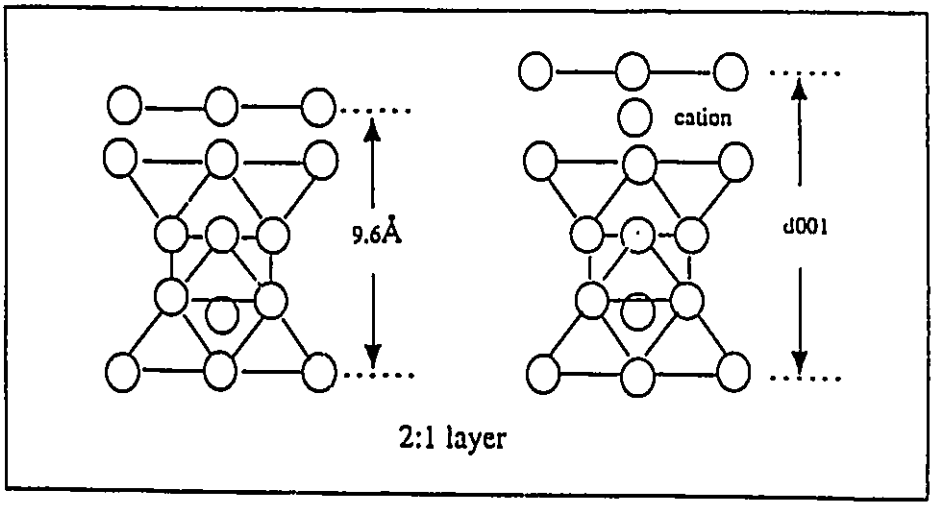

Figure 4.3 Diagrammatic sketch of montmorillonite

Two types of specimen must be considered in the sample preparation in the case of oriented and unoriented samples.[89] A diffractometer patterns from a strongly oriented clay specimen may show only the *00l* series of basal reflection. This kind of patterns is very useful for clay mineral identification, since each basal spacing is related to the type of layer structure involved.[90] Unoriented samples are necessary to obtain complete diffraction data for spacings and intensities. In this research, all the samples prepared for X-ray diffraction were unoriented in order to compare with organo-clay-PDMS membranes. The state of organo-clay in the membrane was considered as unoriented.

Figure 4.4 shows the X-ray diffraction patterns of both oriented and unoriented films of purified Na^+-montmorillonite. On these figures, the intensity of the diffracted X-rays is plotted on the vertical axis against the value of 2Θ. In the spectrum of oriented Na^+-montmorillonite, two strong peaks at d=12.12 Å (2Θ=7.29) and d=4.25 Å (2Θ=28.46) can be attributed to d_{001} and d_{004}. The two broad weak peaks shown at d=6.21 Å (2Θ=14.26) and d=4.25 Å (2Θ=20.87) correspond to d_{002} and d_{003}. From those d_{001} peaks, a value of d_{001}=12.46 Å was calculated. The other small peaks at d=4.47 Å, 3.34 Å, 2.56 Å, 1.49 Å and 1.38 Å (2Θ=19.83, 26.66, 34.97, 62.05, and 68.08) are due to impurities of quartz (2Θ=26.66, 19.83) and NaCl (2Θ=34.97, 62.05, 68.08).[86] The spectrum of unoriented Na^+-montmorillonite shows a similar X-ray diffraction pattern except that the peak for d_{002} is not observed and the value of the maximum of the d_{001} peak (d=11.0 Å) is lower than in the oriented sample. The value of d_{ls} without including d_{002} is calculated to be 2.78 Å which is comparable with the oriented sample.

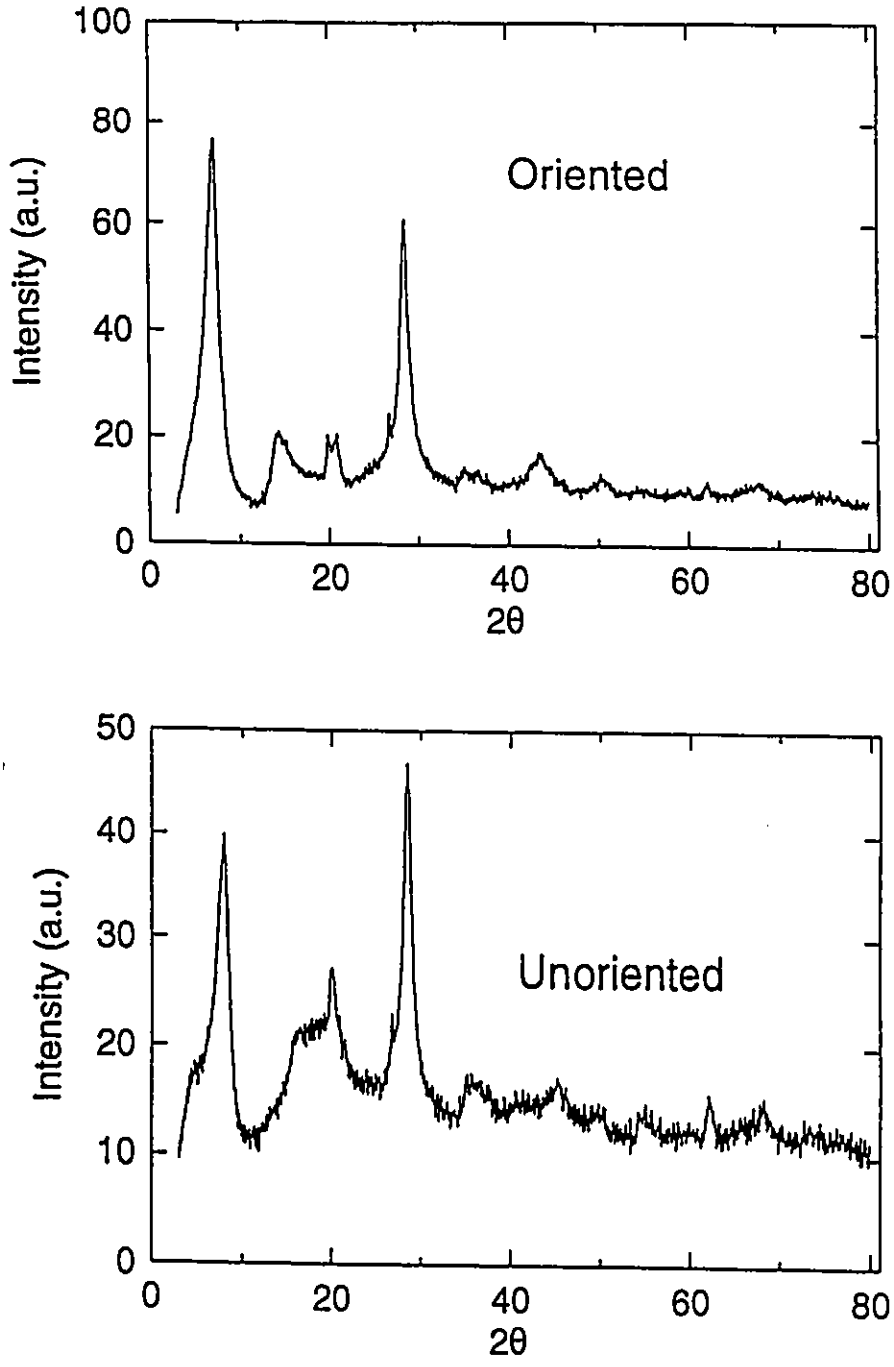

Figure 4.4 XRD spectra for oriented and unoriented Na-montmorillonite samples

Figure 4.5 shows the spectrum of montmorillonite exchanged with the TPP^+ (tetraphenylphosphonium) cation. On this figure, it can be noticed that the d_{001} value shifts to higher value as compared with Na^+-montmorillonite. The d_{is} value for TPP^+-montmorillonite is 8.8 Å. The peaks caused by quartz and NaCl are also observed in the X-ray diffraction pattern of TPP^+-montmorillonite. Another weak peak seen in TPP^+-montmorillonite at about d=1.50 Å is attributed to the d_{060} reflection.[86] The d_{060} diffraction allow the distinction between dioctahedral and trioctahedral types because the b cell dimension is more sensitive to the size of cations and to site occupancy in the octahedral sheet than in a or c dimension. The d_{060} value depends on the composition of the octahedral sheet, the amount of Al in tetrahedral coordination and degree of tetrahedral tilt.[87] The peak at d=1.50 Å (2Θ=61.93) is an intrinsic character of the dioctahedral structure of montmorillonite.

A series of tetraalkylammonium cations ($^+N[(CH_2)_nCH_3]_4$, n = 0, 2, 3, 4, 5, 6) were intercalated into montmorillonite to form organo-clays. From the X-ray diffraction spectra, it was found that there was a gradual increase in the interlayer spacing as the number of carbons in the tetraalkyl chain was increased. When the number of carbon in the tetraalkyl chain increased to five (tetrapentylammonium), there was a jump in the interlayer spacing from 4 - 5 Å to about 8 Å. According to previous studies,[91] this jump is due to the overlap that occurs when organic cations unit charge area is larger than that of montmorillonite (134 $Å^2$). The unit charge area (S_c) represents the surface on a clay layer covered by a single charge which can be expressed as a function of the internal surface (S_i) and CEC:[92]

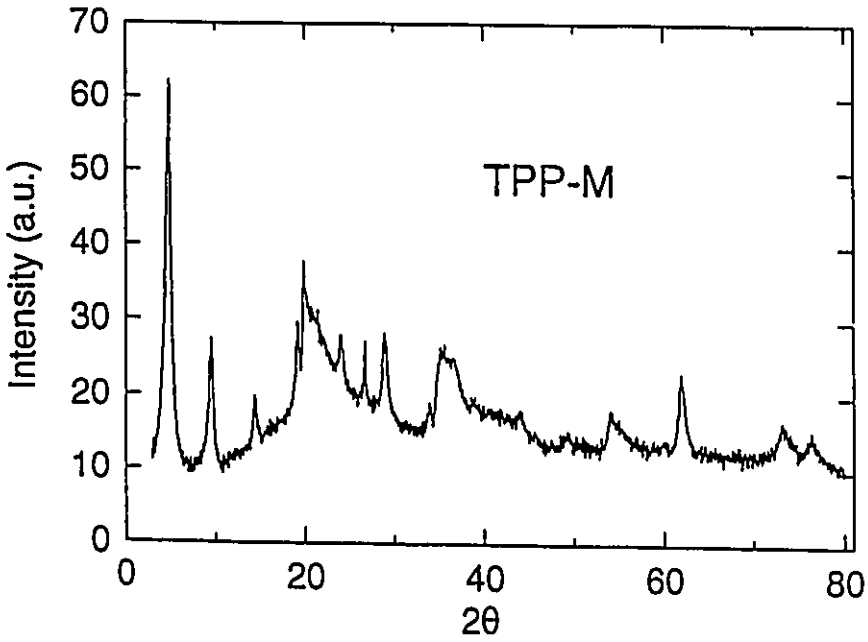

Figure 4.5 XRD spectrum for TPP-montmorillonite

$$S_c = 1000 \cdot S_t / CEC \cdot N_A \qquad (4\text{-}4)$$

where CEC is the cation exchange capacity, expressed in mmoles/g; the unit of S_t is m^2/g and of S_c is m^2. N_A is Avogadro's number. From this relationship, the unit charge area for montmorillonite may be determined as 134 $Å^2$. The surface areas of a series of tetraalkylammonium cations are given in Table 4-1.

Table 4-1 Surface areas of tetraalkylammonium cations

(from tetramethylammonium (TAA1) to tetraheptylammonium (TAA7)

Cation	Surface area (Å²)
TAA1	26
TAA3	78
TAA4	104
TAA5	130
TAA6	156
TAA7	182

The calculation of the cation surface area was based on the following empirical relationship:

$$Cation\ area = N \cdot 26\ \mathring{A}^2 \qquad (4\text{-}5)$$

where N is the number of carbon in each tetraakyl chain, $26\ \mathring{A}^2$ is the surface area of the tetramethylammonium cation, in its flattest configuration, measured on a compact molecular model[3].

Contrary to what was obtained in the X-ray spectrum of TAA1-M, TAA3-M, or TAA4-M, two new peaks at $2\Theta=10.38$ and $2\Theta=15.37$ ($d=8.52$ and 5.76) in the spectra of TAA5-M and TAA7-M indicated bilayer formation. The surface area of TAA5 is 130 Å², which is very close to that of montmorillonite. In this case, the possibility to form bilayer expansion is very small. The observation of bilayer expansion in TAA5-M may be caused by ununiform charge density of montmorillonite. It has been proved that the interlayer

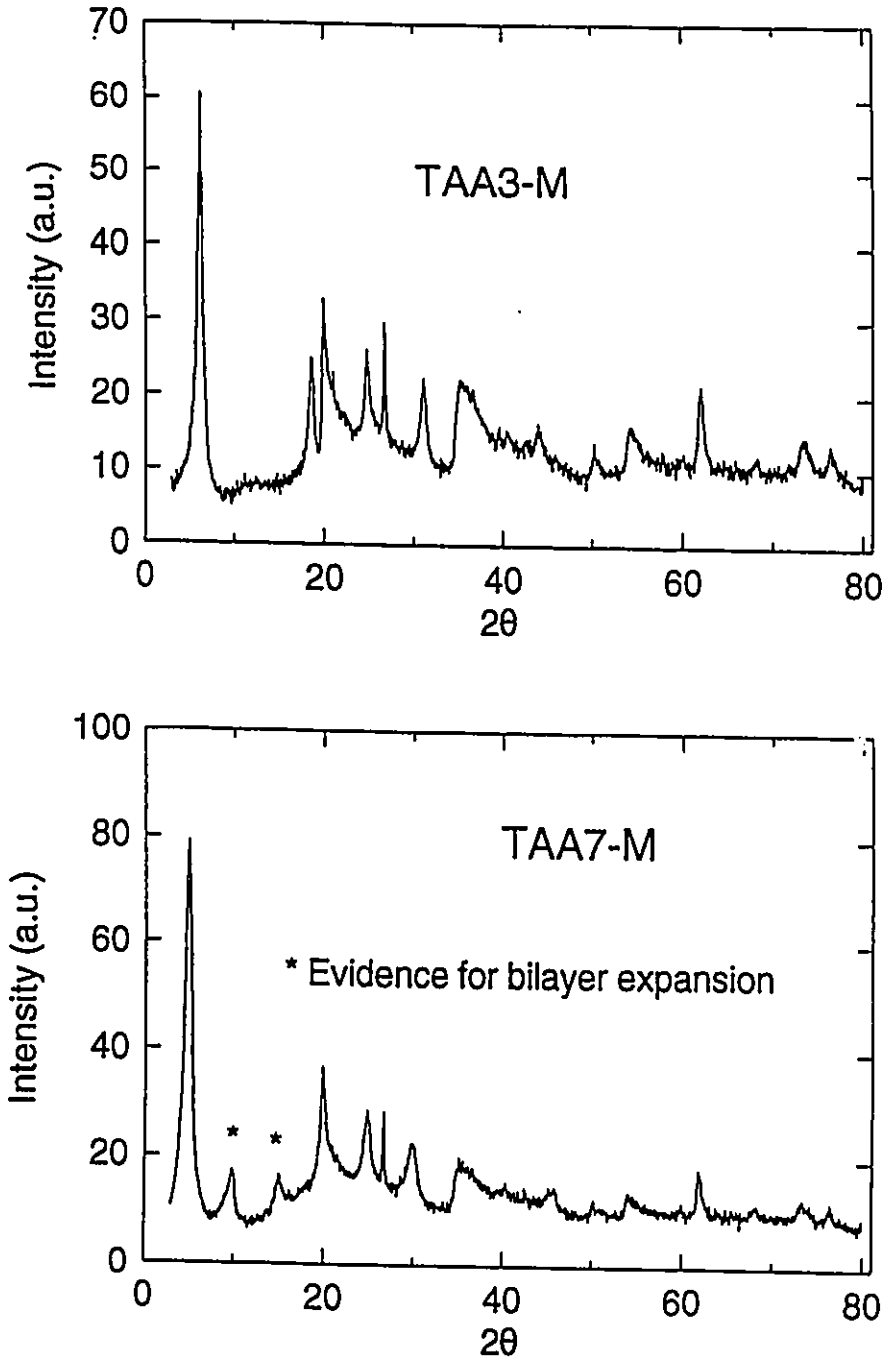

Figure 4.6 XRD spectra for TAA3-M and TAA7-M

spacing of monolayers are mixed-layered with interlayer spacings of bilayer of alkylammonium ions.[93] Such structures can occur only if the cation density varies in succeeding interlayer spaces, being low in interlayer spaces with monolayer and high in interlayer spaces with bilayer. It is possible that the distribution of the charge density in montmorillonite is not uniform. With increasing charge density in certain area, the unit charge area becomes small (< 130 Å^2). In this case, the size of the cation exceeded the available area of the clay to form a bilayer expansion. Figure 4.7 gives the interlayer spacing of exchanged montmorillonite with various tertraalkylammonium cations as a function of the cation size. Figure 4.8 describes the insertion of tetralkylammonium cations with varying surface area in relation to this bilayer expansion.

X-ray diffraction spectra for different organo-clays in PDMS membranes show a very broad peak, due to the polydimethylsiloxane (PDMS) polymer. Figure 4.9 shows the X-ray spectra for a PDMS membrane (PDMS-3) and organo-clay filled PDMS membrane. The d_{ls} value of organo-clays in PDMS are comparable with the value of PDMS free organo-clays. Some d_{ls} value for organo-clays and organo-clays inserted in PDMS are listed in Table 4.2.

Table 4.2 d_{ls} value of some organo-clays and organo-clays in the PDMS

Organo-clays	d_{ls} of organo-clays (Å)	d_{ls} of organo-clay in PDMS (Å)
TPP-M	8.8	8.8
TAA1-M	4.1	4.1
TAA3-M	4.8	4.7

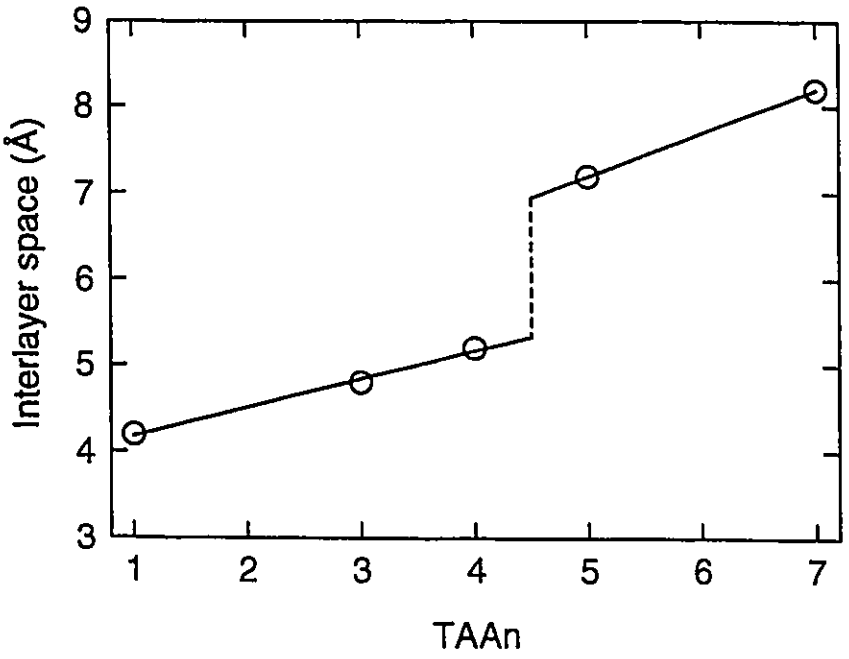

Figure 4.7 **Interlayer spacing of exchanged montmorillonite with TAA cations as a function of the cations size**

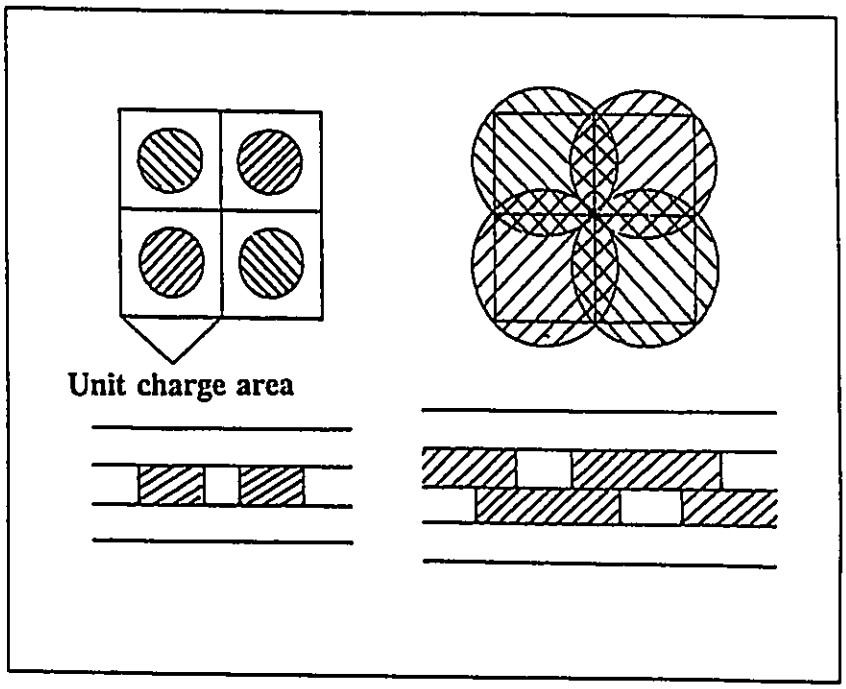

Figure 4.8 **The insertion of TAA cations with varying surface area in relation to bilayer expansion**

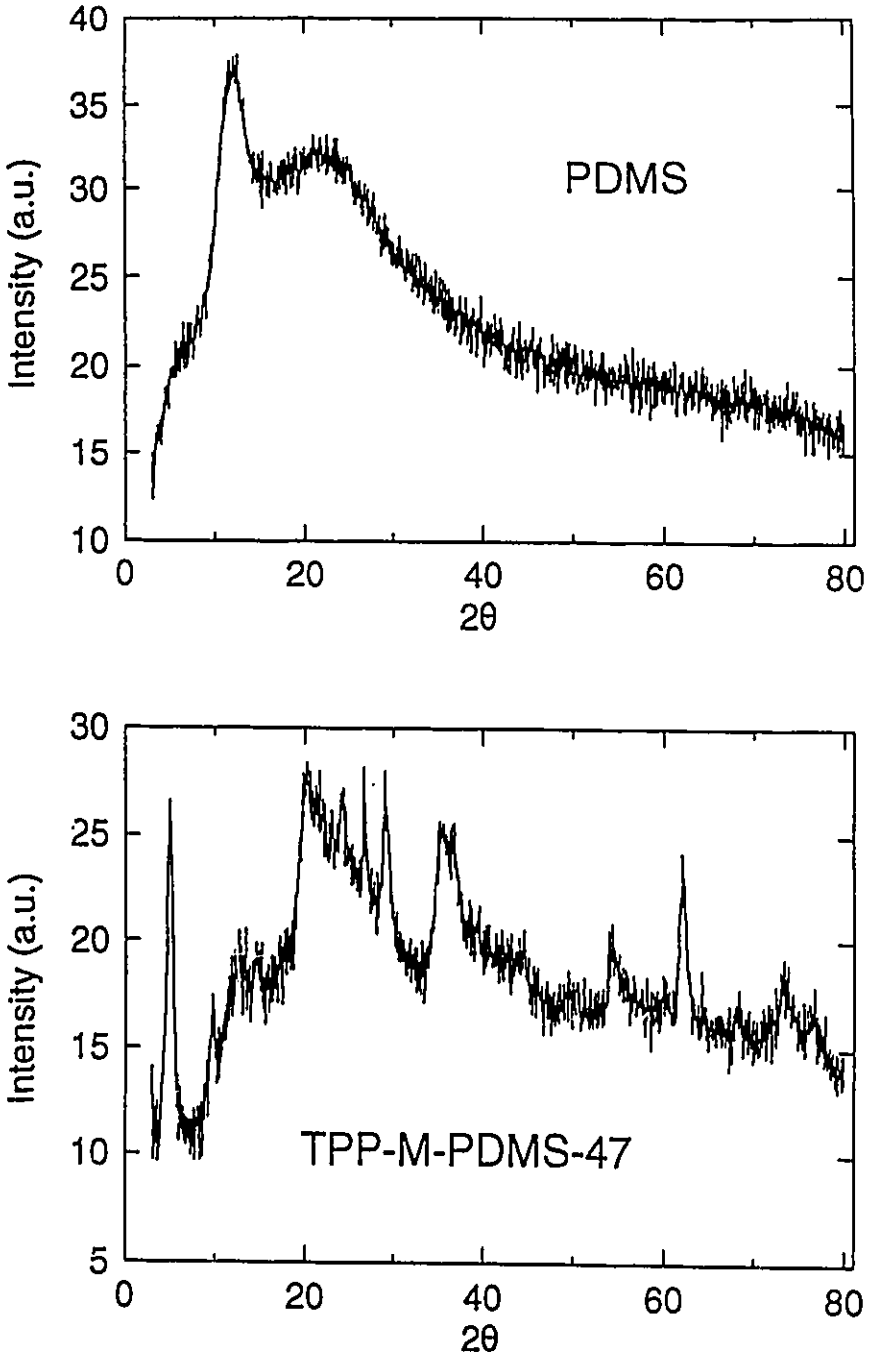

Figure 4.9 XRD spectra of PDMS and organo-clay filled PDMS membranes

4.3 Characterization of the microporosity of organo-clay and organo-clay-PDMS membranes by nitrogen adsorption

Clay materials are candidates as membrane materials, because of their porous structure and of the formation of organic surfaces in the interlayer spaces. The most commonly used procedure for determining porosity and surface area of a powder is to derive the amount of adsorbed nitrogen (or other inert gases) at monolayer coverage from a BET (Brunauer-Emmett-Teller) plot of adsorption isotherm data.[94]

When a solid is exposed in a closed space to a gas or vapor at some definite pressure, the solid adsorbs the gas. The quantity of gas taken up by a sample of solid is proportional to the mass of the sample, and depends also on the temperature T, the pressure p of the vapor and the nature of both the solid and the gas.[95] The quantity (n) of gas adsorbed by the solid can be expressed in moles per gram of solid:

$$n = f(p, T, gas, solid) \qquad (4\text{-}7)$$

For a given gas and temperature, the equation (4-7) can be rewritten as:

$$n = f(p/p_0)_{T,\, gas,\, solid} \qquad (4\text{-}8)$$

p/p_0: relative pressure of gas

where p is the vapor pressure and p_0 is the saturated vapour pressure. Plotting n vs. the relative pressure p/p_0 results in an isotherm. Usually, the adsorption in different cases can

be described by five types of isotherms which are shown in Figure 4.10.[90] Type I and IV are typical isotherms for solids containing microporosity and mesoporosity respectively. Type III describes a non-porous or macroporous solid and type V is given by mesoporous and microporous. Type III and V are characteristic of weak gas-solid interactions. Type II is characteristic of non-porous solid. The stepped isotherm Type VI is rare in practice.

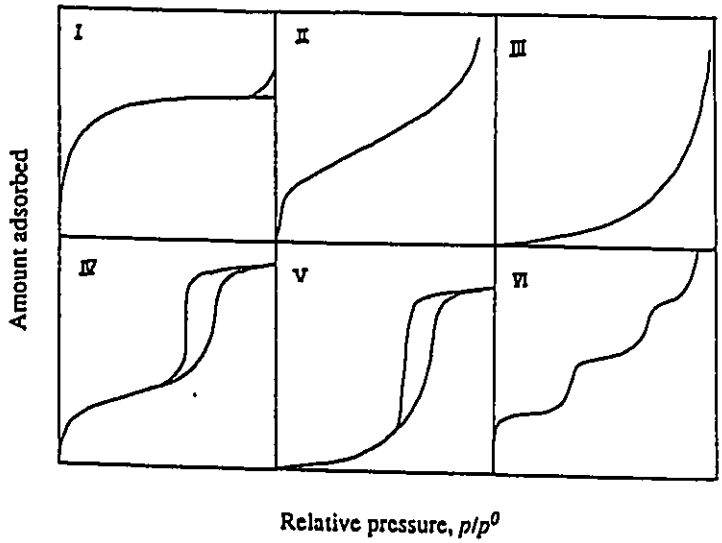

Figure 4.10 Five type of isotherms

Lao[12] has intensively investigated the microporosity of organo-clay minerals, including nitrogen adsorption and desorption isotherms of microporous organo-clays, BET equation and BET surface areas of organo-clays and *T*-plot analysis as well as micropore volumes. The BET model is derived from the non-porous solids which give rise to Type II isotherms. From Type II isotherm, it is possible to calculate the monolayer capacity of a

given gas on particular solid and its specific surface.[94] The monolayer capacity is defined as the amount of adsorbate which can be accommodated in a fully filled, a single molecular layer. The surface area per gram of solid can be given by:

$$S_A = V_m \cdot a_m \cdot N \qquad (4\text{-}9)$$

where S_A is the specific surface area, a_m is the average area occupied by a molecular of adsorbate in the monolayer, N is Avogadro's number and V_m is the monolayer capacity in moles of adsorbate per gram of adsorbent. The total surface area of adsorbent can be calculated from the adsorption isotherm and linearized BET equation which is given by Equation (4-10).[87]

$$p/[V(p_0-p)] = 1/V_m c+[(c-1)/V_m c](p/p_0) \qquad (4\text{-}10)$$

where V is the amount of adsorbate adsorbed in moles per gram of adsorbent , c is the BET constant which is related to the enthalpy of adsorption. Plotting the left side of the equation versus p/p_0 (the relative pressure of adsorbate) results in a straight line. V_m and c can be obtained from the slope and the y-intercept of the liner regression.

$$S(slop) = (c-1)/V_m c \qquad (4\text{-}11)$$

$$I(intercept) = 1/V_m c \qquad (4\text{-}12)$$

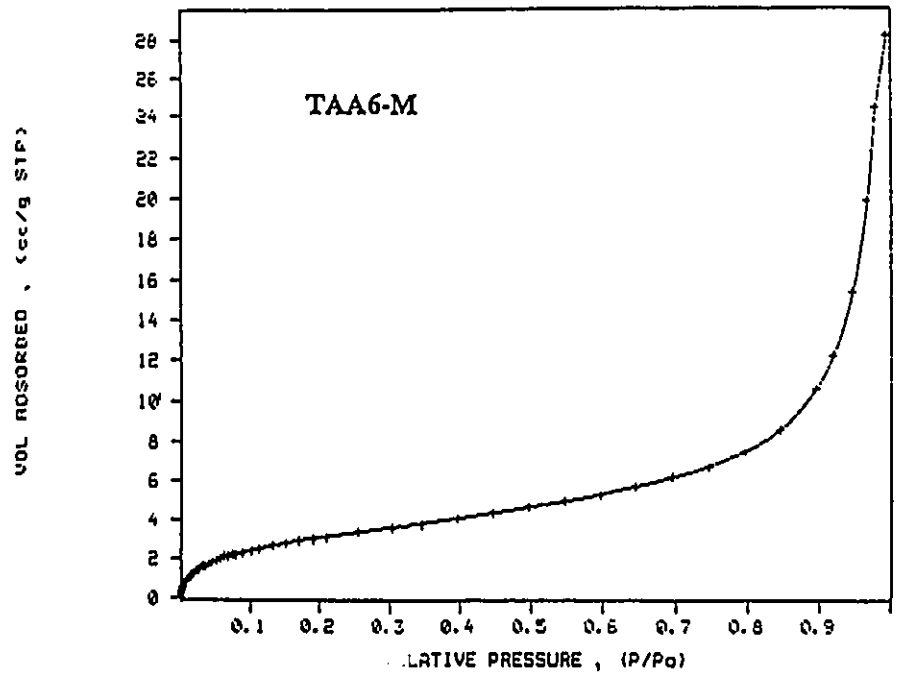

Figure 4.11 Isotherm plot of TAA6-M

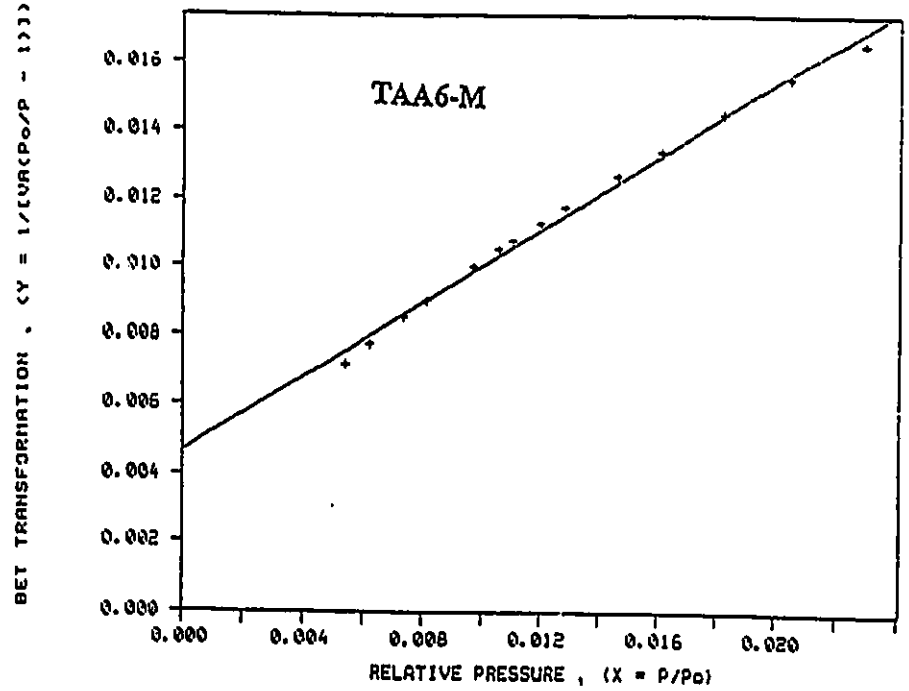

Figure 4.12 BET plot of TAA6-M

The parameters c and V_m are obtained as $c = S/I + 1$ and $V_m = 1/(S + I)$. Therefore, the BET surface area S_A can be calculated using equation (4-9). For nitrogen, a value of 16.2 $Å^2$ for a_m will be used and after applying the appropriate conversion factor, S_A (m^2/g) can be expressed as:

$$S_A = 4.35 \cdot V_m \qquad (4\text{-}13)$$

The total surface area in the solids containing micropores and mesopores can be readily estimated from the BET equation. In this research, BET results of TAA6-M were obtained and shown in Figure 4.11 and 4.12. Figure 4.11 gives the BET adsorption isotherm of TAA6-M. The nitrogen adsorption isotherm is of type II, characteristic of the solid material with non-porous structure. Figure 4.12 gives a graph of BET equation $(P/(P_0-P)v)$ on the y axis against P/P_0 on the x axis gives V_m as the reciprocal of the intercept plus slope. The BET surface areas were calculated assuming the surface area of the nitrogen molecule to be 0.162 nm^2.[12]

Some BET results of organo-clay are given in Table 4.3. The results for TAA1-M and TPP-M were obtained from Lao's research.[12]

Table 4.3 BET surface area, external surface area and interlayer surface area of organo-clays

Organo-clays	BET surface area(m^2/g)	Exterl.surf. area (m^2/g)	Mono-interl. surf.(m^2/g)	Totalinterl. surf.(m^2/g)	Microporsity (%)
TAA1-M	210.3	45.5	164.9	329.8	78
TPP-M	55.9	58.7	0.0	0.0	0
TAA6-M	7.8	-	-	-	0

4.4 Thermal characterization of the organo-clay and of the organo-clay-PDMS membranes by Thermogravimetric Analysis

The TGA graphs of the PDMS membrane, of the organo-clays and of the organo-clay-PDMS membranes are given from Figure 4.13 to Figure 4.15. The TGA of the PDMS membrane given in Figure 4.13 was measured in N_2 and air, respectively. The TGA curve measured in N_2 exhibits a weight loss of 75.5% at roughly 476 °C. At this temperature, the structure of the PDMS polymer is completely destroyed. The corresponding DSC (Differential Scanning Calorimetry) run shows an endothermic transition at 477 °C corresponding to the weight loss of 75.5%. The TGA curve of the PDMS membrane measured in air shows that the PDMS membrane experienced three steps weight loss from 300 °C to 658 °C with 53.3% of total weight loss. The DSC run gives exothermic peaks at 336 °C, 389 °C, 497 °C and 585 °C.

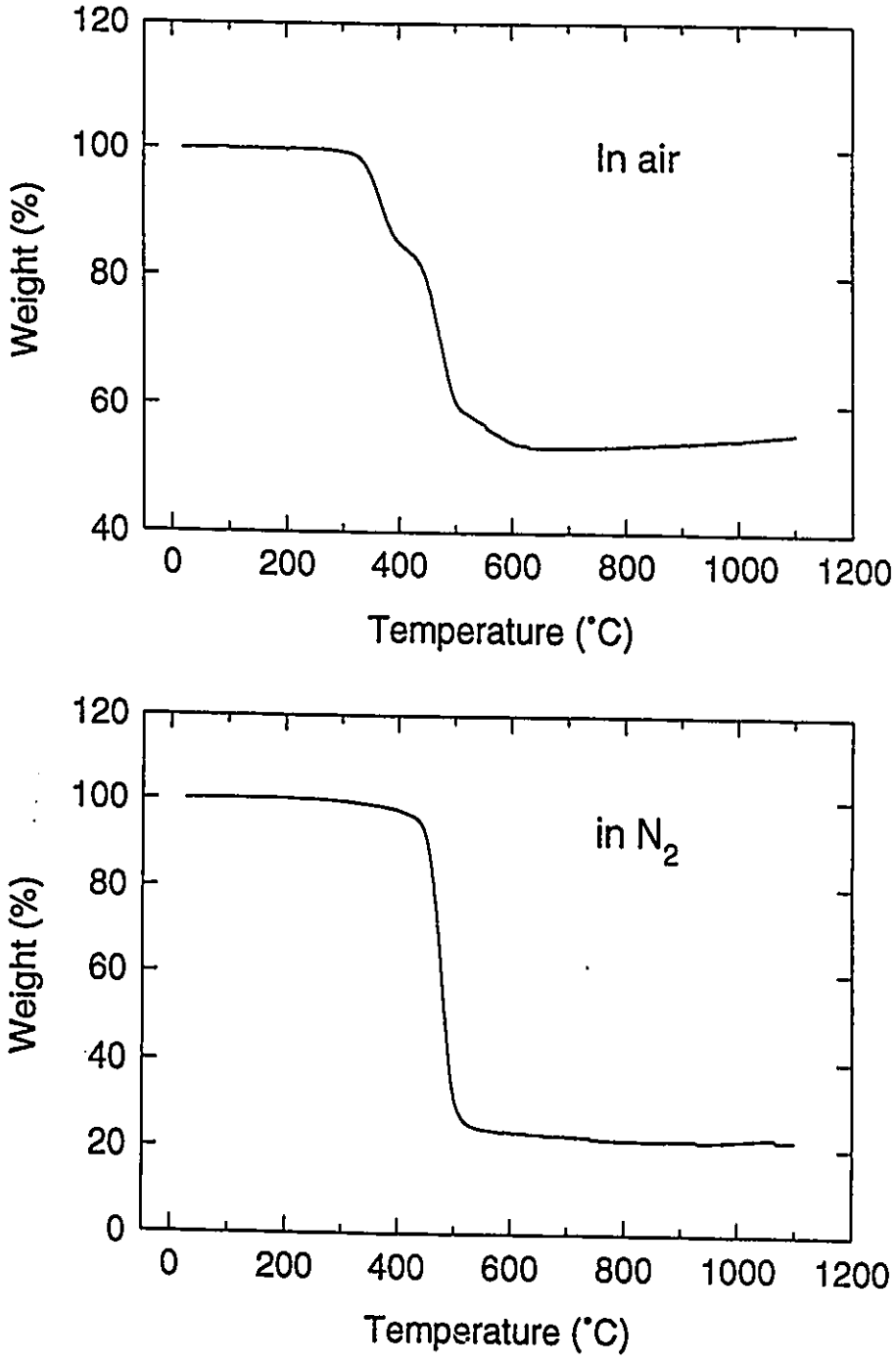

Figure 4.13 TGA of PDMS membrane measured in nitrogen and air

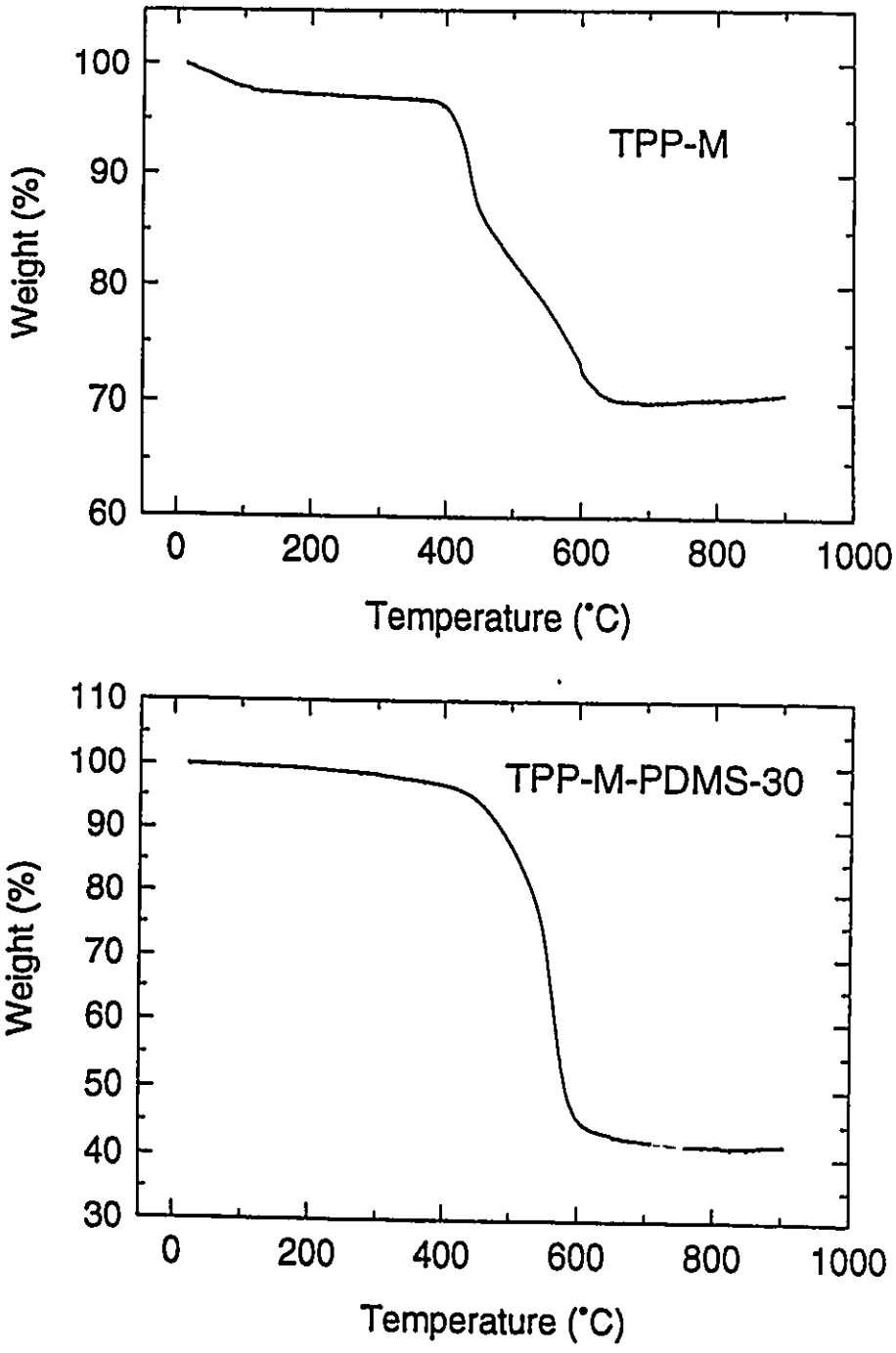

Figure 4.14 TGA of TPP-M and TPP-M-PDMS-30

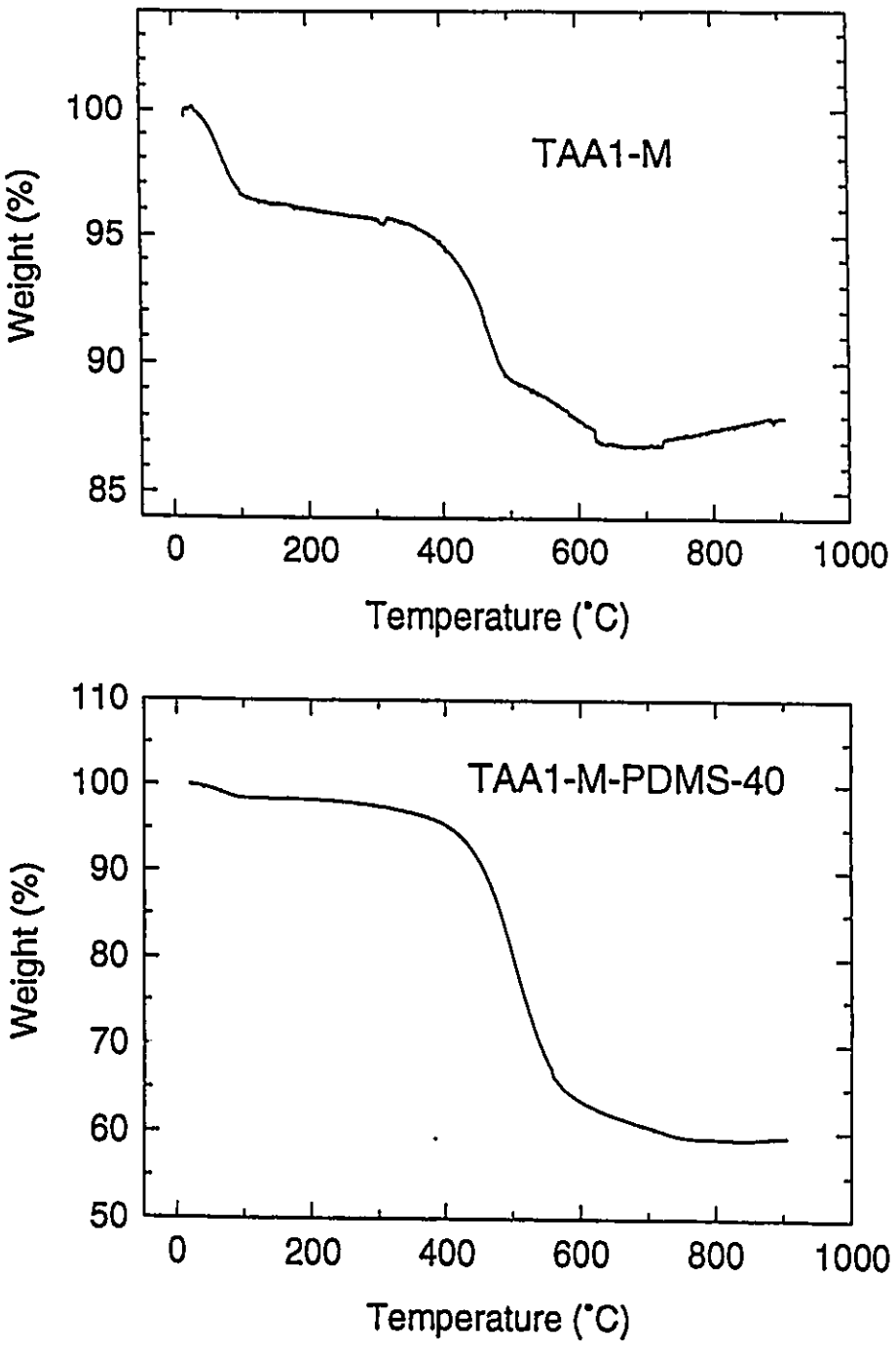

Figure 4.15 TGA of TAA1-M and TAA1-M-PDMS-40

TAA1-M exhibits a weight loss of 3.5% at an onset temperature of 70 °C which corresponds to the loss of surface water. The second decomposition step occurs in the range 300 °C to 490 °C ($T_{ons.}$ =440 °C) with a weight loss of 8.5%, corresponding to the decomposition of organic material. The further slow weight loss of 2.5% from 490 °C to 900 °C was observed, which is due to the decomposition of structural water. Only a single great weight loss is observed in both organo-clay-PDMS membranes except a slight weight loss of surface water in TAA1-M-PDMS-40 membrane. The shape of the graphs is very similar to the shape of the PDMS membrane.

The TGA graphs of TPP-M and TPP-M-PDMS-30 membranes are given in Figure 3.15. TPP-M experienced a abrupt weight loss of 26% from 400 °C to 630 °C after a 4% surface water loss around 100 °C. Actually, two steps weight loss can be observed from 400 °C to 630 °C, but there is no clear boundary between the steps. This might be the combination of the decomposition of organic material and loss of structural water. For both organo-clay-PDMS membranes, the weight loss starts around 400 °C which is lower than that of PDMS membrane and ends at 600 °C. For TAA1-M-PDMS-40 membrane, there is a slow weight loss of 5% after 600 °C. The total weight loss is 40% for TAA1-M-PDMS-40 membrane and 58% for TPP-M-PDMS-30 membrane, respectively.

The TGA results shows that the PDMS and organo-clay-PDMS membranes are thermally stable until about 400°C.

Chapter 5

Performance of Organo-clay-PDMS Composite Membranes in Pervaporation Process

5.1 Introduction

Chlorinated hydrocarbons (CL-HC) are widely used in industrial processes. They are in general toxic and thus constitute a threat for the quality of ground- and surface water. Normally these contaminants are removed by means of one of the following techniques: aeration, ozonisation, adsorption on activated carbon, steam stripping. These techniques all have in general at least one major disadvantage: aeration moves the problems towards air pollution, so that a post-treatment, such as adsorption on activated carbon, is necessary; ozonisation can form new products which are more harmful than the original ones; adsorption on activated carbon is an expensive technique and should therefore only be used with very small quantities of contaminants in the waste water. The major cost of this technique is the regeneration of the activated carbon.

Pervaporation can in principle be used to remove CL-HC from water in an economically interesting way[97]. As mentioned above, adsorption on activated carbon seems

to be most interesting for the removal of very low concentrations of CL-HCs from waste water ($10g/m^3$). For higher concentrations, the cost for regeneration and replacement of the activated carbon filter becomes too high[98], and, consequently, pervaporation becomes one of the least expensive technique.

Benzene is another toxic organic component commonly existing in waste water. There is a great demand for removal of benzene from waste water in many industrial processes. But only a few examples for separation of benzene from benzene/water mixture by pervaporation can be found in literature. Raghunath and Hwang[99] deal with the removal of trace organic compounds including benzene from dilute aqueous solutions by a pervaporation process using tubular PDMS membrane modules. Although their main objective was to emphasize the importance of boundary layer resistance to the transport of various organic species through hydrophobic tubular membrane. A separation factor of 11000 for the removal of benzene from benzene/water mixtures has been reported[53].

The pervaporation experimental results of organo-clay-PDMS membranes for separation of 1,2-DCE and benzene from water are presented in the Chapter. The performance of the organo-clay-PDMS membranes for these separations has been evaluated.

5.2 Separation of 1,2-dichloroethane/water

5.2.1 Pure PDMS Membrane

PDMS as a support material of organo-clay-PDMS membrane played a very important role in this research. As described in chapter 3, the organo-clay-PDMS membranes were

prepared by dispersing organo-clay particles into a PDMS polymeric solution. The effect of PDMS on flux and separation factor must be considered as dealing with the results obtained with organo-clay-PDMS membranes. Therefore, PDMS membranes were measured as references. It also has to be noticed that the values of flux and separation factor obtained with PDMS membrane in pervaporation varied through the literature. The difference between the highest value and the lowest value could span several orders of magnitude. Those differences could be caused by many factors. For example, it could be caused by using PDMS polymers which have different molecular weight and different ending group, by using different experimental system and various measurement methods. As a consequence, the measurement of the pervaporation characteristics of PDMS membranes is a very important part of this research.

Two different thicknesses (50 and 100 μm) of PDMS membrane without any additives were tested. The experimental data for the pure PDMS membranes are given in Table 5.2. As mentioned previously, PDMS membranes are highly selective to organic compounds. The results shown in Table 5.1 indicate that the PDMS membranes are indeed selective to organic compounds. The total flux and 1,2-DCE flux decrease with an increase of membrane thickness, and the separation factors increase with an increase of membrane thickness. The separation factors are 2.0×10^3 and 2.4×10^3 for 50 μm and 100 μm PDMS membranes, respectively.

More test were done on PDMS membrane for separation of 1,2-DCE/water mixtures, with the same equipment, improved and extended from one cell to three cells after ten months. The separation factors of freshly prepared PDMS membranes (PDMS-3) for 1,2-

DCE/water mixtures, 102 μm in thickness, are 1.9 x 10^3 and 1.6 x 10^3 measured by using different cells. Those results are slightly lower than those previously obtained, but they are still in a very comparable range. The performance of organo-clay-PDMS membranes in pervaporation was judged with those values.

Table 5.1 Experimental data for PDMS membranes

Membrane	DCE in feed (X_f)	DCE in permeant (X_p)	Downstr. pressure (torr)	Total flux (g/m^2 h)	DCE flux (g/m^2 h)	α *10^3
PDMS-1	1.4E-05	2.7E-02	2.5	28.9	3.8	2.0
PDMS-2	1.4E-05	3.2E-02	2.5	18.0	2.8	2.4
PDMS-3	1.1E-05	2.0E-02	2.0	24.2	2.5	1.9

5.2.2 Na-montmorillonite-Clay-PDMS Composite Membrane

Table 5.2 shows the experimental results for a Na^+-montmorillonite-PDMS composite membrane. In comparison to PDMS membranes and organo-clay membranes (see below), the 40% montmorillonite-PDMS membrane (with 40% loading: M-PDMS-40) has the highest total flux and the lowest separation factor. These results can be interpreted on the basis of the structure of montmorillonite. As described in Chapter 1, the SWy-1 montmorillonite clay, used for this study, is characterized by a 2:1 layered structure and an expandable interlayer spacing (the distance between two clay layers in a stack). X-ray diffraction pattern indicates that the interlayer spacing of Na^+-montmorillonite is 2.8 Å,

Table 5.2 Experimental data for Na^+-M-PDMS membrane

Membrane	DCE in feed (x_f)	DCE in permeant (x_p)	Downstr. pressure (torr)	Total flux (g/m^2 h)	DCE flux (g/m^2 h)	α $*10^3$
Na^+-M-PDMS-40	1.4E-05	1.2E-02	2.5	34.1	2.1	0.85

corresponding to the thickness of an hydrated sodium cation. When dispersed in water, the clay can swell and intercalate the water layers. When montmorillonite clay is mixed with PDMS and exposed to the mixture solution of 1,2-DCE/H_2O, although PDMS is selective to organic components, the clay adsorbs water preferentially. As a result, the total separation factor for 1,2-dichloroethane/H_2O decreases when Na^+-montmorillonite is inserted in the PDMS membranes.

5.2.3 Organo-clay-PDMS composite membranes

5.2.3.1 Effect of organo-clay content on flux and separation factor

Two types of organo-clay-PDMS membranes, TAA1-M-PDMS and TPP-M-PDMS, with various organo-clay contents were tested in the first series of experiments for investigating the effect of organo-clay content on flux and separation factor. The pervaporation experimental results are listed in Table 5.3 and 5.4. The separation factors of

Table 5.3 The experiment data of TAA1-M-PDMS

Membrane TAA1-M-PDMS	DCE in feed (x_f)	DCE in permeant (x_p)	Downstr. pressure (torr)	Total flux (g/m^2 h)	DCE flux (g/m^2 h)	α $*10^3$
TAA1-20	1.5E-05	2.5E-02	2.5	16.2	2.0	1.7
TAA1-30	1.4E-05	2.0E-02	2.5	22.6	2.3	1.4
TAA1-40	1.4E-05	1.5E-02	2.5	34.6	2.7	1.1

Table 5.4 The experimental data of TPP-M-PDMS

Membrane TPP-M-PDMS	DCE in feed (x_f)	DCE in permeant (x_p)	Downstr. pressure (torr)	Total flux (g/m^2 h)	DCE flux (g/m^2 h)	α $*10^3$
TPP-20	1.3E-05	3.3E-02	2.5	13.9	2.2	2.6
TPP-30	1.5E-05	3.8E-02	2.5	10.4	1.9	2.6
TPP-40	1.4E-05	3.5E-02	2.4	8.1	1.4	2.5
TPP-47	1.4E-05	3.5E-02	2.2	6.4	1.1	2.6

the TAA1-M-PDMS membrane which are lower than the PDMS membrane decrease with an increase of content of TAA1-M from 20% to 40%. While, in the same conditions, the total flux and 1,2-DCE flux decrease with an increase of TAA1-M content to 20%, then increase with an increase of TAA1-M content to 40 %. A slightly higher separation factor than the one observed in the case of the PDMS membrane was systematically obtained with the TPP-M-PDMS composite membrane. In increasing the TPP-M content, both the total flux and the organic component flux decrease, although the separation factor remains approximately constant. Figure 5.1 shows total flux, 1,2-DCE flux and water flux for TAA1-M-PDMS and TPP-M-PDMS membranes. Figure 5.2 gives the summary for the relationship between separation factor and total flux of the tested membranes.

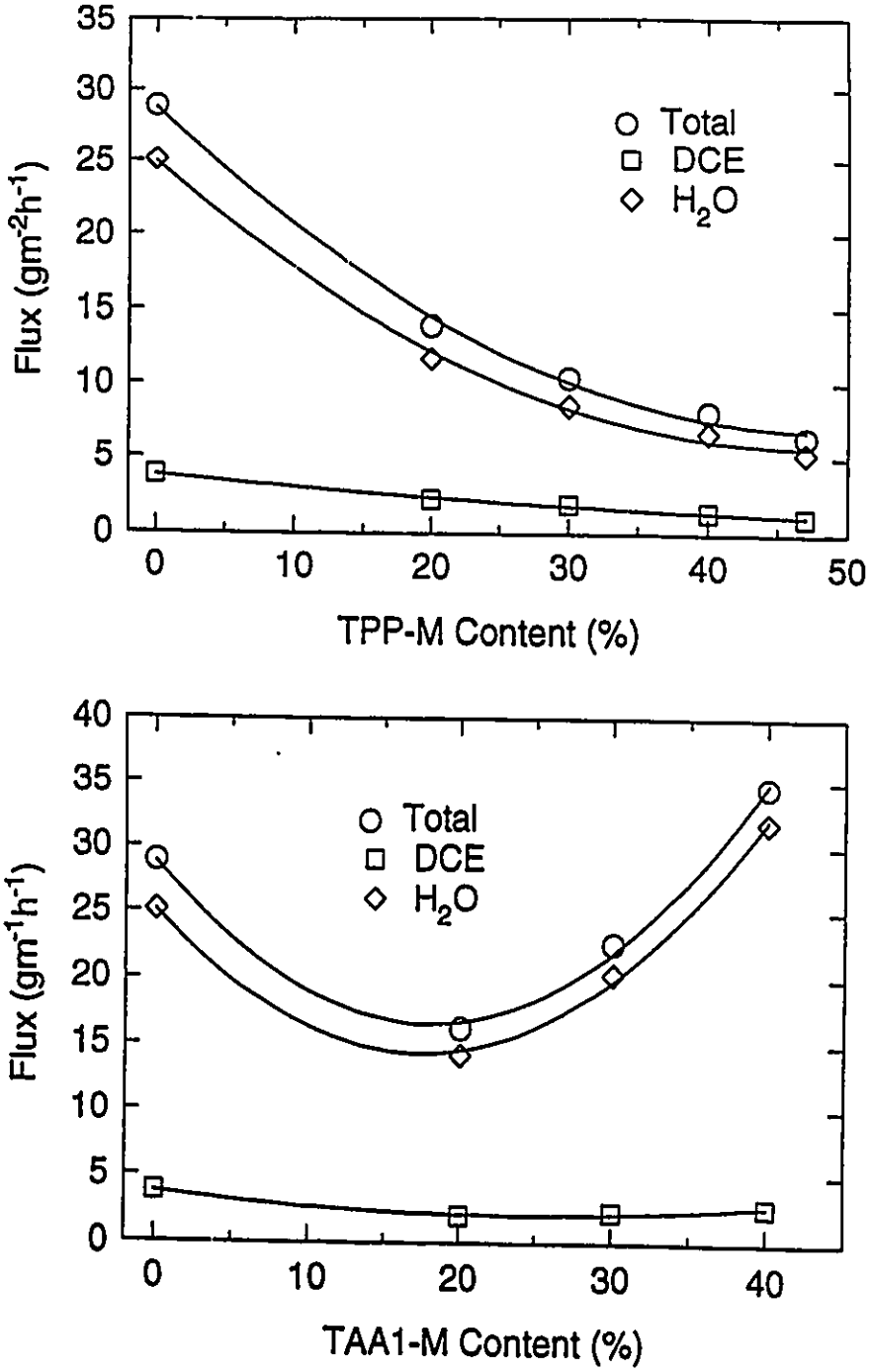

Figure 5.1 **Total flux, 1,2-DCE flux and water flux for TAA1-M-PDMS and TPP-M-PDMS membrane**

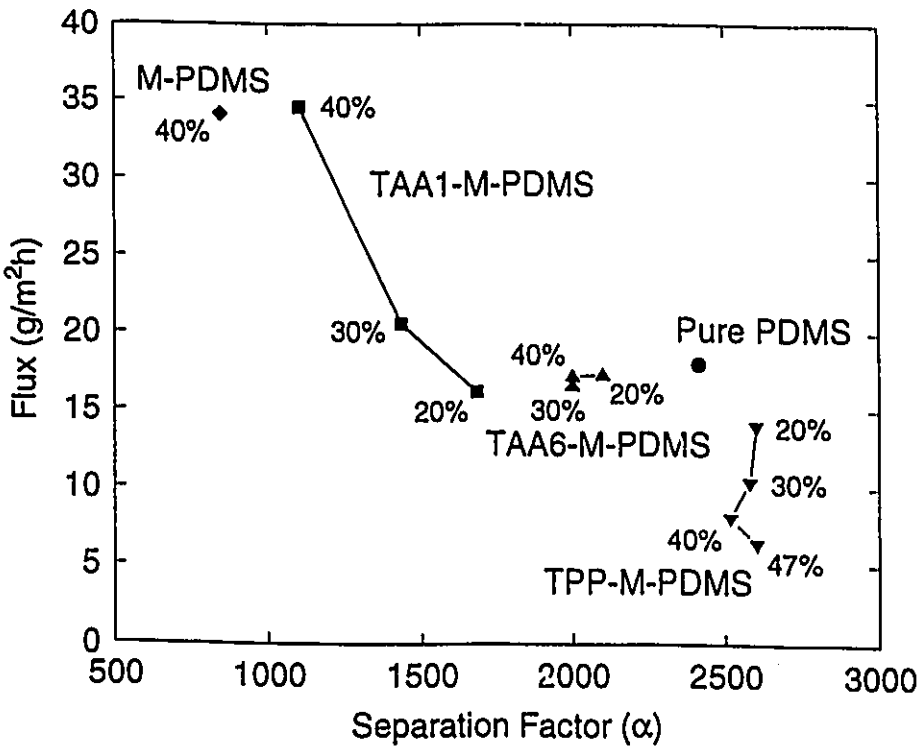

Figure 5.2 **The summary for the relationship between separation factor and total flux of the tested membranes.**

The two different types of organo-clay-PDMS membranes show different performance characteristics in the pervaporation process. The organic phase and the interlayer structure of the organo-clay should have an effect on the separation of 1,2-DCE from water. The structure of the organo-clay resulting from the introduction of different organic cations into the interlayer area of the montmorillonite must be considered.

Due to isomorphous substitution, clay minerals carry a permanent negative charge in their structural framework. The negative charge of the clay layer is counterbalanced by sorption of an equivalent amount of extraneous inorganic cations such as sodium, calcium

and potassium. The inorganic cations in the layer can be replaced by organic cations such as alkylammonium and tetraphenylphosphonium cations. Those cations may cause considerable modifications in the hydrating and swelling properties of the clay. It is well known that clays hold large organic cations more strongly than inorganic cations. The presence of organic cations markedly alters the dispersibility of the clay and practically cancels the clay's ability to swell in water.

The TAA1 cation has a smaller size and covers much less interlamellar clay surface than larger cations. As a result, the free interlayer surface area in TAA1-M organo-clay is large, and is still able to adsorb water through strong dipolar interactions with the available silicate surface. Therefore, although the separation factor of TAA1-M-PDMS membrane is higher than Na-M-PDMS membranes, it is lower than in PDMS membrane. Figure 5.1 shows that the fluxs increase with an increase of the TAA1-M content. This result is in strong support of the above interpretation.

In strong contrast, TPP^+ (area 106 $Å^2$ /ion, as determined from the cross-sectional area of a CPK model) is larger than the silicate surface area available per unit charge (70 $Å^2$ per monolayer clay sheet). The special C_3 orientation of the TPP^+ cation can force the cations to adopt a compact packing inside the interlamellar space of the clay. The nitrogen adsorption results show the absence of any microporousity, indicating that the cations occupy all the interlamellar surface of the clay. Plausibly, this is done by head-to-end stackings, and microporosity can not result from this arrangement in these organo-clays. An organic surface forms once the TPP^+ is introduced to the interlayer of the clay, making the interlamellar spaces very lipophilic. The strong absorption of the organic components in

TPP-M is attributed to these organically covered surface.

For TAA1-M-PDMS membranes, the values of the total flux and of the 1,2-DCE flux indicate that the permeability first decrease with a low TAA1-M content (< 20 w%) added to the membrane. Then, with an increase of the TAA1-M content, the total flux and the 1,2-DCE flux increase. In the resistance model, it is assumed that the component fluxes of both PDMS and of the organo-clay are a function of the organo-clay content of membrane. Obviously the addition of TAA1-M influences the PDMS permeability to some extent. However, the resistance model can not explain why the fluxes experience a minimum point at the addition of 20% TAA1-M. A possible interpretation could be either that the TAA1-M particles act as physical crosslinks for the PDMS phase or that the TAA1-M particles catalyze the chemical crosslinks for the membrane during membrane preparation, or a combination of both effects. This result may arise from the nature of organo-clay used here. At a higher TAA1-M content of the membrane (> 20 w%), this influence gradually vanishes. The flux starts to increase with increasing the TAA1-M content in the membrane. At this point, the resistance model can explain the influence of organo-clay addition on membrane performance. Upon addition of organo-clay, the separation factor is increased because of the high adsorption of 1,2-DCE in TAA1-M, the water flux through the membrane also increases because the surface area in the interlayer spaces of TAA1-M which is not covered by TAA1 cations adsorbs preferentially water. This results in a lower separation factor than for the PDMS membrane.

The 1,2-DCE flux and water flux of TPP-M-PDMS composite membrane decrease with increasing the TPP-M content in the membrane. An abrupt decrease of water flux

results in a increased separation factor. The positive effect of organo-clay content on membrane selectivity results thus from the combined effects of two factors: higher 1,2-DCE adsorption and lower water adsorption in TPP-M.

5.2.3.2 Effect of organic cation size on flux and separation factor

On the basis of the above results, one can conclude that the larger and more hydrophobic organic cation forms a nanocomposite of an organic phase, about 9 Å thick, regularly superimposed with an aluminosilicate phase, also about 9 Å thick. The incorporation of this nanocomposite into PDMS makes the membranes more effective to remove organic components from water by pervaporation.

In previous studies, it has been found that intercalation of tetraalkylammonium cations into montmorillonite could expand the interlayer space of the clay. Since the unit charge area of montmorillonite is 134 $Å^2$, there will be an overlap of the alkyl chains if the cross-sectional area of the inserted cations are larger than 134 $Å^2$. There will be an increase of the interlayer spacing from 4-5 Å to about 8-10 Å (assuming, of course, that cation exchange is complete or nearly complete) to form bilayer structure. In chapter 3, it has been described that the insertion of tetraalkylammonium cations with varying surface areas in relation to this bilayer expansion. Membranes with this type of organo-clay were expected to show higher separation factor for removal of organic components from water because of the formation of large organic nanodomains in the interlamellar spaces of the clay phase. These domains should contribute to the separation of organic component from water.

Table 5.5 and 5.6 show the experimental data of two series of tetraalkylammonium-

montmorillonite-PDMS membranes for the separation of 1,2-DCE/water mixtures by pervaporation. One series was prepared by inserting various tetraalkylammonium ion (from $^{+}NPr_4$ to $^{+}NHep_4$) into the montmorillonite and the membrane was made with containing 50% of those organo-clays. Another series of membranes were prepared by using different content of tetrahexylammonium-clay (20% - 50%). During the test, it was found that the absolute value of the data, separation factor and flux, obtained from cell-1 and cell-3 was quite different for the same membrane. The separation factor obtained from cell-3 was systematically higher than cell-1 with an exception of TAA6. The membranes were tested by series in the same cell, and several membranes were tested in both cells for comparison. The question of the apparent discrepancy between the two cells was discussed in the Chapter of experimental. The Table 5.5 shows the experimental data of different tetraalkylammonium (from $^{+}NPr_4$ to $^{+}NHep_4$)-clay (50%)-PDMS membranes obtained from cell-1. Those data show that the separation factor increased from $^{+}NPr_4$ to $^{+}NHep_4$, but there was no dramatic increase when comparison was made with a pure PDMS membrane. The separation factor for TAA3-M-PDMS was even lower than for PDMS. This result is in good agreement with the working hypothesis of a monolayer structure. The data for TAA1-M-PDMS membrane tested before provide a further evidence for this interpretation. Several membranes were also tested in cell-3, and the results are also given in Table 5.5. Table 5.6 shows the results of tetraalkylammonium-M-PDMS membrane with various organo-clay content tested in cell-3 and cell-1. Increase of the content of organo-clay does not affect strongly the separation factor.

Table 5.5 Experimental data for TAAn-M-PDMS-50

(tested by cell-1)

Membrane TAAn-M-PDMS	DCE in feed (X_f)	DCE in permeant (X_p)	Downstr. pressure (torr)	Total flux (g/m^2 h)	DCE flux (g/m^2 h)	α $*10^3$
PDMS	1.1E-05	1.7E-02	1.8	18.1	1.6	1.6
TAA1-M-47-1	1.4E-05	1.5E-02	2.5	34.6	2.7	1.1
TAA3-M-50-1	1.1E-05	1.0E-02	2.1	21.6	1.2	1.0
TAA4-M-50-2	1.0E-05	1.5E-02	1.4	7.9	0.6	1.4
TAA5-M-50-2	1.0E-05	1.5E-02	1.4	4.3	0.3	1.5
TAA6-M-50-1	9.7E-06	1.6E-02	1.3	2.3	0.2	1.7
TAA7-M-50-1	9.3E-06	1.6E-02	1.4	7.9	0.7	1.8

(tested by cell-3)

Membrane TAAn-M-PDMS	DCE in feed (X_f)	DCE in permeant (X_p)	Downstr. pressure (torr)	Total flux (g/m^2 h)	DCE flux (g/m^2 h)	α $*10^3$
PDMS	1.1E-05	2.0E-02	2.0	24.2	2.5	1.9
TAA3-M-50-2	9.7E-06	1.1E-02	2.3	32.1	1.8	1.1
TAA5-M-50-1	1.1E-05	2.3E-02	1.3	20.7	2.4	2.2
TAA6-M-50-1	9.9E-06	1.2E-02	2.3	41.1	2.6	1.1

Table 5.6 Experimental data for TAA6-M-PDMS

(tested by cell-3)

Membrane TAA6-M-PDMS	DCE in feed (X_f)	DCE in permeant (X_p)	Downstr. pressure (torr)	Total flux (g/m^2 h)	DCE flux (g/m^2 h)	α *10^3
PDMS	1.1E-05	2.0E-02	2.0	24.2	2.5	1.9
TAA6-M-20-3	8.8E-06	2.0E-02	1.7	17.3	1.7	2.1
TAA6-M-30-3	1.0E-05	2.0E-02	1.6	17.2	1.8	2.0
TAA6-M-40-2	1.0E-05	2.0E-02	1.6	16.6	1.7	2.0
TAA6-M-50-1	9.9E-06	1.2E-02	2.3	41.1	2.6	1.1

(tested by cell-1)

Membrane TAA6-M-PDMS	DCE in feed (X_f)	DCE in permeant (X_p)	Downstr. pressure (torr)	Total flux (g/m^2 h)	DCE flux (g/m^2 h)	α *10^3
PDMS	1.1E-05	1.7E-02	1.8	18.1	1.56	1.6
TAA6-M-20-1	1.1E-05	1.7E-02	1.6	10.4	0.91	1.7
TAA6-M-20-2	1.1E-05	1.4E-02	1.5	10.3	0.76	1.4
TAA6-M-20-1	1.1E-05	1.01-02	2.0	14.5	0.83	1.1
TAA6-M-50-1	9.7E-06	1.6E-02	1.3	2.3	0.20	1.7

5.2.3.3 Effects of feed temperature and permeate pressure

Some of the membranes have been tested for small change of the feed temperature and of the downstream pressure. The results are listed in Table 5.7. They show that the separation factor remains constant with a changing in both temperature and pressure. The

total flux slightly decreased with an increase of the downstream pressure and increased with an increase of the temperature. Probably, higher temperature, about 40-50 °C, should be tested in future experiments.

Table 5.7 The effects of feed temperature and downstream pressure on the flux and the separation factor

Membrane	Temperature (°C)	Pressure (torr)	Total flux (g/m^2 h)	DCE flux (g/m^2 h)	α $*10^3$
Pure PDMS (cell-1)	22.03	1.76	18.14	1.56	1.6
	22.07	5.00	13.45	0.92	1.4
	28.18	2.07	21.86	1.58	1.3
TAA6-M-PDMS-30-1 (cell-3)	21.73	2.03	30.52	2.53	1.5
	21.64	5.00	25.17	1.96	1.7
	27.75	2.30	35.05	2.58	1.4
TAA6-M-PDMS-20-2 (cell-3)	21.60	2.00	30.31	3.35	2.1
	21.47	5.00	26.15	2.42	2.1
	27.70	2.00	33.98	3.48	2.0
	27.81	5.00	30.39	2.53	1.9
TAA6-M-PDMS-50-1 (cell-3)	21.68	2.30	41.08	2.56	1.1
	27.75	3.11	52.30	2.51	1.0
TAA3-M-PDMS-50-1 (cell-1)	22.01	2.11	21.63	1.16	1.0
	21.87	5.00	18.55	0.83	1.0
	28.13	2.02	33.84	1.64	0.9
	28.03	5.00	34.57	1.38	0.9

5.2.3.4 *Membrane Reproducibility and Experimental Duration*

Two 40% organo-clay-PDMS membranes made from different sheet of TAA1 and TPP organo-clay-PDMS membranes were tested for flux and separation data reproducibility. The results are listed in Table 5.8. They confirm reproducibility of the experimental data.

Since the transport mechanism in organo-filled PDMS membranes is not elucidated, an hypothesis was emitted, that the observed high selectivity of the membranes is a phenomenon attributable to initial adsorption by the organo-clay, and that it would disappear when a steady-state would be obtained. To prove the high selectivity to be an intrinsic property of this type of membrane, a long-run pervaporation test was conducted. A duration experiment was performed using a TPP-M-PDMS-20 membrane. From Table 5.9, it can be seen that a 3 hours testing period may be adequate for each membrane. This provides rather convincing evidence that the 1,2-DCE molecules adsorbed in organo-clay and diffuse through the crystallites and desorb on the permeate side.

Table 5.8 Membrane reproducibility

Membrane	DCE in feed (X_f)	DCE in permeant (X_p)	Downstr. pressure (torr)	Total flux (g/m^2 h)	DCE flux (g/m^2 h)	α $*10^3$
TAA1-M-PDMS-40%-1	1.4E-05	1.5E-02	2.5	34.6	2.7	1.1
TAA1-M-PDMS-40%-2	1.3E-05	1.4E-02	2.5	41.9	3.0	1.1
TPP-M-PDMS-40%-1	1.5E-05	3.7E-02	2.4	6.2	1.1	2.5
TPP-M-PDMS-40%-2	1.4E-05	3.5E-02	2.4	8.1	1.4	2.5

Table 5.9 Experimental duration with 20%-TPP-M-PDMS membrane

Time (min)	DCE in feed (X_f)	DCE in permeant (X_p)	Downstr. pressure (torr)	Total flux (g/m^2 h)	DCE flux (g/m^2 h)	α $*10^3$
30	1.4E-05	3.3E-02	2.3	17.9	2.8	2.5
60	1.4E-05	3.3E-02	2.4	16.1	2.6	2.5
120	1.3E-05	3.2E-02	2.4	16.2	2.5	2.5
240	1.3E-05	3.2E-02	2.3	16.2	2.5	2.6
330	1.2E-05	3.1E-02	2.3	16.3	2.4	2.5

5.3 Separation of benzene/water mixtures

5.3.1 The membranes were tested in system 1

5.3.1.1 PDMS and TPP-M-PDMS membranes

A 6 hour testing period for each membrane was applied for the separation of benzene/water mixture, because of the small effective membrane area (10.2 cm^2) in the system 1. The test was repeated to ensure that the correct results have been collected. Table 5.10 shows the separation of the benzene/water mixtures by using a PDMS membrane. The value of 11.8 for separation factor could be reached in the beginning of the test, with a flux of 20.8 g/m^2 h. When the test was repeated with the same membrane, the separation factor decreased, while the total flux remained approximately constant.

Table 5.10 Separation of benzene/water mixture by pure PDMS membrane in system 1

Membrane: Pure PDMS Thickness: 107 μm

Numbers of operation	Benz. in feed (X_f)	Benz. in permeant (X_p)	Total flux ($g/m^2 h$)	α
1	9.4E-05	1.1E-03	20.8	11.8
2	10.2E-05	1.7E-03	19.7	16.4
3	6.6E-05	4.7E-04	19.6	7.1
4	7.9E-05	4.6E-04	19.0	5.8

The decrease of separation factors could also be found in the case of TPP-M-PDMS membranes. The pervaporation experimental data for TPP-M-PDMS membranes are given in Table 11. The results show that the separation factor of TPP-M-PDMS-20 and TPP-M-PDMS-47 membranes decreased with a repetition of the test, but it remained constant for TPP-M-PDMS-30 and TPP-M-PDMS-40 after the second operation. The total flux of TPP-M-PDMS membranes remained unchanged with a repetition of the test except TPP-M-PDMS-20 membrane. For TPP-M-PDMS-20 membrane, the increase of total flux could be caused by the defect of the membrane.

Based on those results, it is difficult to draw a real conclusion on the performance of TPP-M-PDMS membranes for separation of benzene/water mixtures. According to the XRD results, the TPP-M parts in the TPP-M-PDMS membranes remained unchanged before and after the pervaporation test. The decrease of separation factor indicates that the PDMS and PDMS part in the TPP-M-PDMS membranes was not stable with benzene/water mixture. This unstable may be caused by benzene adsorption and membrane swelling. Although the

results for TPP-M-PDMS -30 and TPP-M-PDMS-40 membranes remain constant, more repetitions are needed to make any real conclusion on their stability. The insufficient efficacy of system 1 may result in very low separation factor comparing to the system 2 (see Table 13) and the values reported in the literature.

Table 5.11 Separation of benzene/water mixture by TPP-M-PDMS membranes in system 1

Membrane: TPP-M-PDMS-20 Thickness: 79-94 μm

Number of operation	Benz. in feed (X_f)	Benz. in permeant (X_p)	Total flux (g/m^2 h)	α
1	6.8E-05	2.5E-03	17.1	36.0
2	6.1E-05	8.7E-04	23.8	14.4
3	5.8E-05	8.4E-04	29.4	14.5
4	6.8E-05	7.1E-04	41.4	10.4
5	4.6E-05	1.7E-04	75.8	3.8
6	8.9E-05	4.2E-04	110.4	4.7

Membrane: TPP-M-PDMS-30 Thickness: 100 μm

Numbers of operation	Benz. in feed (X_f)	Benz. in permeant (X_p)	Total flux (g/m^2 h)	α
1	7.7E-05	2.6E-03	16.3	34.0
2	7.2E-05	2.5E-05	15.0	35.5

Membrane: TPP-M-PDMS-40 **Thickness: 76 μm**

Numbers of operation	Benz. in feed (X_f)	Benz. in permeant (X_p)	Total flux (g/m^2 h)	α
1	5.4E-05	2.3E-03	21.5	43.1
2	5.0E-05	2.1E-03	22.4	42.3

Membrane: TPP-M-PDMS-47 **Thickness: 105 μm**

Numbers of operation	Benz. in feed (X_f)	Benz. in permeant (X_p)	Total flux (g/m^2 h)	α
1	4.7E-05	1.9E-03	11.6	40.7
2	5.7E-05	6.8E-04	12.1	12.0
3	8.6E-05	2.6E-03	13.6	30.2
4	8.1E-05	1.5E-03	12.6	18.1

However, TPP-M-PDMS membranes give much higher separation factor for separation of benzene/water mixture than PDMS membranes. This means that the positive effect of the addition of organo-clay on membrane properties. These results further confirm that the organic surface formed in the interlayer spacing by intercalating TPP cation indeed contribute to the separation of organic compounds from water. An increase in separation factor for benzene from 11.8 for the organo-clay free PDMS membrane to about 40 for a membrane with 47% TPP-M in PDMS membrane probably results from a combination of both the enhanced sorption of benzene into the membrane and the fast transport through the membrane.

5.3.1.2 TAA6-M-PDMS membranes

The experimental data of TAA6-M-PDMS membranes are given in Table 5.12. The results show that the separation factor and total flux of the membranes increase with the number of test performed, and the general trend of the separation factor was in the opposite direction compared with PDMS or TPP-M-PDMS membranes.

Table 5.12 Separation of benzene/water mixture by TAA6-M-PDMS membranes in system 1

Membrane: TAA6-M-PDMS-50-1 Thickness: 85-90 μm

Numbers of operating	Benz. in feed (X_f)	Benz. in permeant (X_p)	Total flux (g/m^2 h)	α
1	7.8E-05	6.8E-04	30.5	8.8
2	6.4E-05	4.4E-04	33.4	6.9

Membrane: TAA6-M-PDMS-50-2 Thickness: 100 μm

Numbers of operating	Benz. in feed (X_f)	Benz. in permeant (X_p)	Total flux (g/m^2 h)	α
1	1.2E-04	5.1E-04	37.2	4.1
2	4.6E-05	3.1E-04	45.9	6.7
3	5.4E-05	3.7E-04	47.1	6.8
4	6.3E-05	7.3E-04	41.3	11.6
5	6.6E-05	1.2E-03	47.5	10.3

5.3.2 The TAA-M-PDMS membranes were tested in system 2

Some preliminary experimental data have been obtained with the equipment at McMaster University by using benzene/water mixture as feed solution. The results are shown in Table 5.13 They are only roughly calculated, since the measurement system was not optimized for this feed mixture. However, they give a semi-quantitative picture of how the tested organo-clay-PDMS membranes are effective in separation of benzene/water mixture.

The pure PDMS membrane and TAA-M-PDMS membranes have slightly higher separation factor for benzene/water mixture separation than for 1,2-DCE/water mixture. The absolute values of the separation factors obtained on both systems are not directly comparable, since the measurements were done with a vary different approach. However, they give generally the same trends.

Table 5.13 Separation of benzene/water mixture by TAA-M-PDMS membrane in system 2

(Benzene/water mixture)

Membrane TAA6-M-PDMS (cell)	BENZ.in feed (X_f)	BENZ.in permeant (X_p)	Downstr. pressure (torr)	Total flux (g/m^2 h)	BENZ. flux (g/m^2 h)	ß *10^3
PDMS-3 (1)	2.7E-05	5.0E-02	1.8	20.4	4.6	2.0
TAA6-40-4 (1)	2.9E-05	5.6E-02	1.8	17.8	4.4	2.1
TAA6-50-1 (1)	4.5E-05	9.2E-02	1.4	12.4	4.4	2.2
TAA3-50-2 (3)	4.5E-05	5.6E-02	2.8	-	-	1.3
TAA6-20-1 (3)	2.9E-05	7.6E-02	1.8	-	-	2.8
TAA6-40-1 (3)	2.9E-05	7.3E-02	1.7	-	-	2.9

Chapter 6

Conclusion

The present work opens a way to improve the pervaporation separation characterization of PDMS membrane by introducing organo-clays into PDMS.

Organo-clay-PDMS composite membranes were prepared by mixing several types of organo-clay materials with polydimethylsiloxane. They were tested for the separation of 1,2 DCE/water and benzene/water mixtures by pervaporation.

The overall permeation and separation factors are functions of the organo-clay content and of the nature of the organo-clay. The maximum separation factor achieved for benzene/water mixtures was about 40 with TPP-M-PDMS membrane. This is three times higher than with pure PDMS membranes. In the case of DCE/water mixtures, the separation factor was increased by using an hydrophobic organo-clay, a nanocomposite material resulting from the incorporation of tertraphenylammonium cations in the interlayer spaces of montmorillonite. This material is made of organic nanophases, about 9 Å thick. Further studies should focus on increasing the hydrophobicity and the local fluidity of these organic nanophases in the PDMS matrix.

A resistance model was used to explain the transport through the organo-clay-PDMS composite membrane. The transport phenomena in the pervaporation with organo-clay-PDMS membranes are more complex than in the case of polymeric membranes.

References

1. A.G. Cairns-Smith and H. Hartman, "*Clay minerals and the origin of life*", Cambridge University Press, New York, 1986.
2. H. van Olphen, "*An Introduction to Clay Colloid Chemistry*", 2nd Ed., John Wiley & Sons, New York, 1977.
3. L. Mercier, *B.Sc Honours Thesis*, Department of Chemistry, University of Ottawa, 1991.
4. G. Lagaly, *Solid State Ionics*, **22** (1986) 43.
5. R.E. Grim, *Clay Mineralogy*, 2nd: McGraw-Hill: New York, 1969.
6. R.M. Barrer and A.D. Millington, *J. Colloid Interface Sci.*, **25** (1967) 359.
7. M. Harper and C.J. Purnell, *Environ. Sci. Technol.*, **24**(1) (1990) 55.
8. H. Lao, S. Latieule and C. Detellier, *Chem. Mater.*, **3** (1991) 1009.
9. R.M. Barrer and G.S. Perry, *J. Chem. Soc.*, (1961) 842.
10. R.M. Barrer and G.S. Perry, *J. Chem. Sci.*, (1961) 850.
11. J.F. Lee, M.M. Mortland S.A. Boyd and C.T.Chiou, *J. Chem. Soc., Faraday Trans.*, 1, **85** (1989) 2953.
12. H. Lao, *PhD Thesis*, Department of Chemistry, University of Ottawa, 1993.
13. G.Villemure, *Clays and Clay Minerals*, **38** (1990) 622

14. J.F. Lee, M.M. Mortland, C.T. Chiou, D.E. Kile and S.A. Boyd, *Clays and Clay Minerals*, **38** (1990) 113.

15. S.A. Boyd, S, Shaobai, J.F.Lee and M.M. Mortland, *Clays and Clay Minerals*, **36** (1988) 125.

16. K.R. Srinivasan and H.S. Fogler, *Clays and clay minerals*, **38** (1990) 287.

17. K.R. Srinivasan and H.S. Fogler, *Clays and clay minerals*, **38** (1990) 277.

18. F. Call, J. Sci. *Food. Agric.*, **8** (1957) 630.

19. J.J. Jurinak, *Soil Sci. Amer. Proc.*, **21** (1957) 599.

20. C.T. Chiou and T.D. Shoup, *Environ. Sci. Technol.*, **19** (1985) 1196.

21. M.B. McBride, T.J. Pinnavaia and M.M. Mortland, *Adsorption of aromatic molecules by clays in aqueous suspension:* in Fate of Pollutants in the Air and Water Environments, Part 1, Vol. 8, I. H. Suffet, Ed., Wiley, New York, 145

22. T.A. Wolfe, T. Demirel and E.R. Baumann, *Clays and Clay Minerals*, **33** (1985) 301.

23. S.A. Boyd, J.F. Lee and M.M. Mortland, *Nature*, **333** (1988) 345.

24. D. White and C.T. Cowan, *Trans. Faraday Soc.*, **54** (1958) 557.

25. J.L. McAtee and B.R. Harris, *Clays and clay Minerals*, **25** (1977) 90.

26. S.A. Boyd, M.M. Mordland and C.T. Chiou, *Soil. Sci. Soc. Amer. J.* **52** (1988) 652.

27. P.M. Chapman, G.P. Romberg and C.A. Vigers, *J. Water Pollution Control Fed.*, **54** (1982) 292.

28. K.R. Srinivasan and H.S. Fogler, E.G. Gulari, T.F. Nolan and J.S. Schuttz, *Environ. Progress*, **4** (1985) 239.

29. H.F. Fogler and K.R. Srinivasan, *U.S. Patent 4,740,488*, April 26, 1988.

30. Y. Yan and T. Bein, *Chem. Mater.*, **5** (1993) 905.

31. L.J. Michot and T.J. Pinnavaia, *Clays and Clay Minerals*, **38** (1990) 634.

32. W.S. Winston Ho and K.K. Sirkar, *Membrane Hanbook*, Van Nostrand Reinhold, New York, 1992.

33 R.Y.M. Huang, *Pervaporation Membrane Separation Processes*, Elsevier, 1991.

34. H.J.C. te Hennepe, D. Bargeman, M.H.V. Mulder and C.A. Smolders, *J. Membrane Sci.*, **35** (1987) 39.

35. H.J.C. te Hennepe, C.A. Smolders, D. Bargeman and M.H.V. Mulder, *Sep. Sci. Technol.*, **26** (1991) 585.

36. H.J.C. te Hennepe, D. Bargeman, M.H.V. Mulder and C.A. Smolders, *Stud. Suef. Sci. Catal.*, **39** (1988) 411.

37. M. Jia, K.V. Peinemann and R.D. Behling, *J. Membrane Sci.*, **57** (1991) 289.

38. M. Goldman, D.Frankel and G. Levin, *J. Appl. Polym. Sci.*, **37** (1989) 1791.

39. H.J.C. te Hennepe, W.B.F. Boswerger, D. Bargeman, M.H.V. Mulder and C.A. Smolders, *J.Membrane Sci.*, **89** (1994) 185.

40. P.A. Kober, *J. Am. Chem. Soc.*, **39** (1917) 944

41. L. Farber, *Science*, **82** (1935) 158.

42. E.G. Heissler, A.S. Hunter, J. Sciliano and R.M. Treadway, *Science*, **124** (1956) 77.

43. R.C. Binning, R.J. Lee, J.F. Jennings and E.C. Martin, *Ind. Eng. Cham.*, **53** (1961) 45.

44. S. Loeb, *Desalination by reverse osmosis*, V. Merten Ed., M.I.T. Press. Cambridge

Mass., U.S.A., 1966. Chap. 3, p.55.

45. S. Loeb and S. Sourirajan, *Adv. Chem. Ser.*, **38** (1962) 117.

46. S. Leob and S. Sourirajan, *U.S. Pat., 3,133,132.*, May 12, 1964.

47. A.H. Ballweg, H.E.A. Brüschke, W.H. Schneider, G.F. Tusel, K.W. Böddeker and A. Wenzlaff, *Communication. Fifth Internat. Sympos. on Alcohol Fuel Technology.*, Auckland, New Zaeland, May 13-18, 1982.

48. H.E.A. Büschke, W.H. Schneider and G.F. Tusel, K.W. Böddeker and A. Wenzlaff, *Communication. European Workshop on Pervaporation.* Nancy, France, Sept. 21-22, 1982.

49. G.F. Tusel and A. Ballweg, *U.S. Pat. 4,405,409.* Sept. 20, 1983.

50. H.E.A. Büschke, *Proc. 3rd Int. Conf. on Pervaporation Processes in Chemical Industry*, R. Bakish Ed., Bakish Materials Coep., Englewood N.J. (1988) 2.

51. J. Kaschemekat, J.G. Wijmans, R.W. Baker and I. Blume, *Third Internat. Confer. on Pervaporation Processes in the Chem. Industry.* Nancy, France, Sept. 19-22, 1988.

52. Hans O.E. Karlsson and Gun Trägårdh, *J. Membr. Sci.*, **76** (1993) 121.

53. H. Eustache and G. Histi, *J. Membr. Sci.*, **8** (1981) 105.

54. G. Bengtson, K.W. Böddeker, H.P. Hanssen and I. Urbasch, *Biotechnol. Tech.*, **6** (1992) 21.

55. Y. Morigami, M. Kondo and A. Kidoguchi, *in Proc. 2nd Int. Conf. on Pervaporation Processes in the Chemical Industry, Bakish Materials Corporation,* Englewood, NJ, **200** (1987) 208.

56. P. Aptel and J. Nell, *Pervaporation. In Synthetic Membranes: Science, Engineering, and Application*, Dordrecht, Holland: D. Reidel Publishing Company (1986) 403.

57. A.S. Michaels, R.F. Baddour, H.J. Bixler and C.Y. Choo, *Ind. Eng. Chem. Proc. Deg. Develop.*, **1** (1962) 14.

58. V.N. Schrodt, R.F. Sweeny and A. Rose, *Division of Industrial and Engineering Chemistry, 144th Meeting*, ACS, Los Angeles, March 1963.

59. R.B. Long, *Ind. Eng. Chem. Fundamentals.*, **4** (1965) 445.

60. S. Sourirajan, B. Shiyao and T Matsuura, *Proceedings of the 2nd International Conference on Pervaporation processes in Chemical Industrial*, San Antonio, Texas, March 8-11, R. Bakish ed. (1987).

61. S. Sourirajan and T. Matsuura, *Reverse Osmosis an Ultrafiltration process principles*, National Research Council of Canada, Chapter 4, (1985).

62. M. Yoshikawa, H. Yokoi, K. Sanui and N. Ogata, *J. Polym. Sci.*: Polym Chem. Ed., **22** (1984) 473.

63. M. Yoshikawa, H. Yokoi, K. Sanui and N. Ogata, *J. Polym. Sci.*: Polym Chem. Ed., **22** (1984) 125.

64. M. Yoshikawa, H. Yokoi, K. Sanui and N. Ogata, *J. Polym. Sci.*: Polym Chem. Ed., **22** (1984) 2159.

65. M. Yoshikawa, T. Yukoshi, K. Sanui and N. Ogata, *J. Polym. Sci.*: Polym Chem. Ed., **22** (1986) 1585.

66. M. Yoshikawa, N. Ogata and T. Shimitzu, *J. Membrane Sci.*, **18** (1974) 351.

67. B. Raghunath and S.-T. Hwang, *J. Membrane Sci.*, **75** (1992) 29-46.

68. J.M.S. Henis and M.K. Tripodi, *Sep. Sci. Technol.*, **15** (1980) 1059.

69. J.M.S. Henis and M.K. Tripodi, *J. Membrane Sci.*, **8** (1981) 233.

70. J.M.S. Henis and M.K. Tripodi, *Science*, **220** (1983) 11.

71. A. Fouda, Y. Chen, J. Bai and T. Matsuura, *J. Membrane Sci.*, **64** (1991) 263.

72. H.H. Nijhuis, *Ph.D. thesis*, University of Twente, Enschede, The Netherland, 1990.

73. R.M. Barrer, J.A. Barrie and N.K. Raman, *Rubber Chem., Technol.*, **36**(3) (1963) 651.

74. K. Polmanteer, *Rubber Chemistry and technology*, **52** (1979) 454.

75. C. Bartels-Caspers, E. Tusel-Langer and R.N. Lichtenthaler, *J. Membr. Sci.*, **70** (1992).

76. R.W. Grose and E.M. Flanigen, (Union Carbide), *U.S. Pat. 4,061,724*, (1977).

77. M. Jia, K.V. Peinemann and R.D. Behling, *J.Membrane Sci.*, **73** (1992) 119.

78. R. Tyagi, *PhD Thesis*, Department of Chemical Engineering, University of Ottawa, (1993).

79. R.Y.M. Huang and C.K. Yeom, *J. Membrane Sci.*, **58** (1991) 33

80. (a) R. Barrer and D.M. Macleod, *Trans. Farady Soc.*, **51** (1955) 1290. (b) R.M. Barrer and J.S.S Reay, *Trans. Faraday Soc.*, **53** (1957) 1253. (c) R.M. Barrer and G. Hampton, *Trans. Faraday Soc.*, **53** (1957) 1462. (d) R.M. Barrer, *Pure Appl. Chem.*, **61** (1989) 1903. (e) R.M. Barrer, *Clays and clay Miner.*, **37** (1989) 386.

81. A.C. Zettlenoyer, *J. Phys. Chem.*, **59** (1955) 962.

82. A.C.D. Newman, "*Chemistry of Clays and Clay Minerals*", Chap. 6, Mineralogical Society, 1987

83. S. Latieule, *Master's Thesis*, Department of Chemistry, University of Ottawa, (1991).

84. J.M. Adams, *J. Inclusion Phen.*, **5** (1987) 663.

85. E.W. Nuffield, *"X-Ray Diffraction methods"*, John Wiley and Sons, Inc., New York, (1966).

86. D.M. Moore and R.C. Reynolds, Jr., "*X-Ray Diffraction and the Identification and Analysis of Clay Minerals*", Oxford University Press, 1989.

87. M.J. Wilson, "*A Handbook of Determinative methods in Clay Mineralogy*", (1987).

88. J.M. Serratosa, J.A. Rausell-Colom and J. Sanz, *J. Mole. Catal.*, **27** (1984) 225.

89. H. V. Olphen and J.J. Fripiat, "*Data Handbook for Clay Materials and Other Non-Metallic Minerals*", Pergamon Press, 1979.

90. G.W. Brindley, *Crystal Structure of Clay Minerials and Their X-Ray Identification, Chapter 2*, Ed. G.W.Brindley and G. Brown, Mineralogical Society, London (1980).

91. A.C. Olis, P.B. Malla and L.A. Douglas, *Clay Minerals*, **25** (1990) 39.

92. L. Mercier and C. Detellier, *Clays and Clay Minerals*, **42** (1994) 71.

93. J.L. McAtee, Clays and Clay Minerials, **5** (1958) 279.

94. S. Brunauer, P.H. Emmett and E. Tellar, *J. Amer. Chem. Soc.*, **60** (1938) 309.

95. S.J. Gregg and K.S.W.Sing, *Adsorption, Surface area and Porosity*, Academic Press Inc.Second Edition, (1982)

96. K. Rilling, *Final report to ICST*, Department of Chemical Engineering, McMaster University, (1994)

97. I. Blume and C.A. Smolders, *Seminar Application of Membrane Processes in Evironmental Problems*, Maastricht, 1991.